A New Perspective on Battery-Electric Aviation, Part II: Conceptual Design of a 90-Seater

Reynard de Vries*, Rob E. Wolleswinkel†,
Elysian Aircraft, Rendementsweg 2, 3641SK Mijdrecht, The Netherlands

Maurice F. M. Hoogreef‡ and Roelof Vos§
Delft University of Technology, Kluyverweg 1, 2629HS Delft, The Netherlands

Battery-electric aviation is commonly believed to be limited to small aircraft and is therefore expected have a negligible impact on the decarbonization of the aviation sector. In this paper we argue that, with the correct choice of design parameters and top-level aircraft requirements, the addressable market is actually substantial. To demonstrate this, the Class-II sizing of a battery-electric 90-seater is performed, and the environmental impact is assessed in terms of well-to-wake CO_2-equivalent emissions per passenger-kilometer. The resulting 76-ton aircraft achieves a battery-powered useful range of 800 km for a pack-level energy density of 360 Wh/kg. For this range, it has an energy consumption of 167 Wh per passenger-kilometer and an environmental impact well below that of kerosene, eSAF, or hydrogen-based aircraft alternatives and comparable to land-based modes of transport. These results indicate that, to successfully reduce the climate impact of the aviation sector, battery-electric aircraft should not be designed as a niche product operating from small airfields but as commercial transport aircraft competing with fuel-based regional and narrowbody aircraft.

Nomenclature

AEO	=	All engines operative	C_D	=	Drag coefficient, $D/(0.5\rho V^2 S)$ [-]
BM	=	Battery mass	C_{D0}	=	Zero-lift drag coefficient [-]
CASK	=	Cost per available seat-kilometer	C_L	=	Lift coefficient, $L/(0.5\rho V^2 S)$ [-]
DoD	=	Depth of discharge	$C_{L,\max}$	=	Maximum lift coefficient [-]
ECS	=	Environmental control system	D	=	Drag [N]
EoL	=	End of life	D_{fus}	=	Fuselage diameter [m]
eSAF	=	Synthetic (power-to-liquid) SAF	e	=	Oswald factor [-]
eVTOL	=	Electric vertical take-off and landing	h	=	Altitude [m]
EV	=	(Ground based) electric vehicle	l	=	Tail moment arm [m]
HT	=	Horizontal tail	L	=	Lift [N]
IPS	=	Ice protection system	l_{fus}	=	Fuselage length [m]
LTO	=	Landing and take-off cycle	M	=	Mach number [-]
MTOM	=	Maximum take-off mass	N	=	Number of propellers [-]
OEI	=	One engine inoperative	P_{s}	=	Shaft power [W]
OEM	=	Operating empty mass	Q	=	Interference factor [-]
PLM	=	Payload mass	S	=	Wing planform area [m²]
PMAD	=	Power management & distribution	s_{L}	=	Landing distance [m]
RAM	=	Regional air mobility	s_{TO}	=	Take-off distance [m]
SAF	=	Sustainable aviation fuel	T	=	Thrust [N]
STOL	=	Short take-off and landing	V	=	Flight speed [m/s], volume [m³]
TMS	=	Thermal management system	V_{app}	=	Approach speed [m/s]
VT	=	Vertical tail	W_{TO}	=	Maximum take-off weight [N]
A	=	Wing aspect ratio [-]	η_{p}	=	Propeller efficiency [-]
b	=	Wing span [m]	ρ	=	Ambient air density [kg/m³]

*Head of Design & Engineering, reynard@elysianaircraft.com, AIAA member.
†Co-CEO and CTO, rob@elysianaircraft.com, AIAA member.
‡Assistant Professor, Faculty of Aerospace Engineering, m.f.m.hoogreef@tudelft.nl, AIAA member.
§Associate Professor, Faculty of Aerospace Engineering, r.vos@tudelft.nl, Associate Fellow AIAA.

I. Introduction

Different pathways are currently being investigated to reduce the climate impact of the aviation sector [1]. Many studies conclude that electric aircraft are only feasible for very short ranges (200~400 km) with both current and future battery technology (200~500 Wh/kg) [2–5]. This has led to the common perception of battery-electric aviation being limited not only to short ranges, but also to small aircraft. In this two-part paper series, we challenge this perspective to show that, with the right design choices, the useful range achievable with batteries is substantially higher than literature suggests. And while the range is still significantly lower than fuel-based aircraft, this increase justifies a fundamental shift in perspective regarding the potential role of battery-electric propulsion in the decarbonization of the aviation sector: rather than designing electric aircraft for niche or emerging markets, they can be designed to compete with large fuel-based aircraft.

Here, the concept of "large fuel-based aircraft" refers to aircraft in the CS-25/FAR Part 25 category with more than e.g. 50 seats: regional turboprops, regional jets, narrowbodies, and widebodies. These aircraft cover the vast majority of passenger-kilometers travelled by air and are also responsible for the majority of aviation-related emissions [5, 6]. Among these aircraft types, the narrowbodies—and not the regionals—dominate the market on short ranges (< 2000 km) [7]. This is largely driven by their low cost per available seat-kilometer (CASK) compared to regional jets and turboprops, as a result of their higher passenger count and flexibility to also operate on longer routes within the airline's network. Thus, to maximize the impact of electric aviation on the sector as a whole, electric aircraft would have to be designed to compete with aircraft such as the Airbus A320neo and Boeing 737MAX in terms of operating costs, while achieving a useful range which is as high as possible.

Part I of this paper series [8] describes four key design principles that enable an increase in the useful range of electric aircraft. First, electric aircraft have a high empty mass but a low empty mass *fraction* (where "empty mass" excludes the batteries). This is a result of their intrinsically high energy mass (i.e. battery mass) fraction. Second, electric aircraft inherently have a high lift-to-drag ratio due to their low wetted-area-to-reference-area ratio. Third, using a fuel-based reserve energy system to cover reserves is a much lighter solution than to carry that energy in the form of batteries, without impacting the day-to-day emissions and energy costs of the aircraft. And finally, increasing the passenger count of an electric aircraft does not limit its range. To the contrary—for the same energy efficiency, designing an electric aircraft for more passengers often leads to an increase in maximum range.

This follow-up paper, Part II, has two purposes: to verify these design principles by performing a more in-depth design of an electric aircraft, and to demonstrate that the impact of such aircraft on the climate footprint of the aviation sector can be substantial. For this, the question is not: "How do we design an electric aircraft to mimic existing aircraft as much as possible and fit into existing networks?" But, instead: "What should the top-level requirements and operations of such an aircraft look like, if we want to maximize the decarbonization potential of this new technology?" Therefore, rather than providing the design requirements as input, we first discuss how they are selected in Sec. II. Then, in Sec. III, the conceptual design of a battery-electric aircraft is performed for the selected set of requirements. Finally, Sec. IV performs an environmental comparison to other means of transport. In this process, we identify a series of technical challenges that must be addressed in the development of such aircraft, which are finally summarized in the Conclusions (Sec. V).

II. Selection of Top-Level Aircraft Requirements

A. Design Objective

The design objective is to achieve an aircraft with zero emissions during day-to-day operation which can operate cost-effectively and from the same airports as narrowbodies. With this objective in mind, the top-level aircraft requirements and aircraft configuration were iteratively evaluated. The following sections describe the top-level aircraft requirements which were finally selected.

B. Payload-Range Requirements

When designing an aircraft, most mass (and CASK) contributions scale less than linearly with payload mass. As a result, increasing the passenger count is generally beneficial for the energy efficiency per passenger-kilometer. There are, however, several reasons why it is not practical to indefinitely increase the number of passengers, such as market considerations (insufficient demand to cover a route effectively), infrastructure considerations (e.g. airport span constraints), physical limits (e.g. square-cube law [9]), or technology availability (e.g. components for multi-MW,

multi-kV electrical power transmission). Based on these considerations and preliminary calculations for 19, 40, and 90-seater configurations, a payload requirement of 90 passengers is selected. In this trade-off, the airport gate span constraint is found to play a particularly important role, as evidenced in earlier work [10].

Contrary to fuel-based aircraft, where the harmonic range for which the aircraft is designed is based on economic considerations and not on physical limitations of the maximum range, for electric aircraft maximizing the achievable range is key to ensure a large market potential (see Sec. IV.D). Thus, in this study we investigate what battery characteristics would be required to reach a 1000 km target, and then assess which ranges are achievable with more "near-term" battery technologies (see Sec. III.C). Moreover, for reserves, three components are considered: diversion range, loiter time, and contingency. These are covered by a dedicated fuel-based reserve energy system. The aircraft is therefore technically a hybrid, although it is described here as "battery-electric" since it only uses the reserve energy system for emergencies. Thirty minutes loiter and 5% contingency are assumed to be applicable based on current regulations [11]. Note that, while it is unclear whether electrically-driven large aircraft will have to satisfy a 30 mins or 45 mins loiter time, this does not appreciably affect the design proposed in this paper due to the use of a fuel-based reserve energy system. For the diversion to alternate, a range of 150 km is assumed, flown at $M = 0.4$ and 1800 m altitude. These values are summarized in Table 1.

Table 1 Summary of main top-level aircraft requirements.

Parameter	Value	Parameter	Value
Number of passengers [-]	90	AEO climb gradient [-]	8%
Mass per passenger [kg]	100	Contingency energy [-]	5%
Range (target) [km]	1000	Diversion range [km]	150
Take-off field length [m]	2000	Diversion Mach number [-]	0.4
Landing distance [m]	2000	Diversion altitude [m]	1800
Approach speed [m/s]	74.6	Loiter time [mins]	30
Cruise Mach number [-]	0.6	Battery charging time [mins]	<45
Cruise altitude [m]	>7000	Wing span at gate [m]	<36

C. Performance Requirements

Unlike gas turbines and reciprocating engines, electric motors do not present a power lapse with altitude. As a result, the installed power is generally constrained by the take-off distance requirement (see Sec. III.A.6). Reducing the power required for take-off and climb is therefore key to reducing the powertrain mass, which is especially important given the high powertrain mass fraction of (hybrid-)electric propulsion systems [12]. In other words, a longer take-off distance is more beneficial for the empty-mass fraction of an electric aircraft than for a turbofan or turboprop aircraft. We therefore argue that, for maximum energy efficiency, the electric aircraft should be designed for the same "long" runways as narrowbody aircraft, and not for small airfields.

Based on this, a typical narrow-body take-off distance of 2000 m is selected as take-off balanced field length and as landing distance requirement. This is contrary to most design studies on electric aviation, which generally size the aircraft to match the take-off and landing distance of turboprop aircraft [13, 14], or even for short take-off and landing (STOL) capabilities [15]. Given the amount of narrowbody-compatible runways in regions like Europe and North America, we hypothesize that the reduction in empty weight fraction—and thus, the increase in range and energy efficiency—enabled by a "long" runway is more relevant for the overall market potential of the electric aircraft, than the ability to operate from airfields with runways below 2000 m length. This implies that the aircraft will not be able to compete with e.g. turboprop aircraft on specific routes. Moreover, to limit the approach speed to values corresponding to existing large passenger aircraft, an approach speed of 145 kts (74.6 m/s) is specified.

The cruise speed is selected to be as high as possible, while remaining in the subsonic regime to allow for aerodynamically-efficient unswept wings and propeller propulsion. This trade-off results in a cruise Mach number requirement of $M = 0.6$. From an operational perspective one could argue that the cruise speed should be derived from a block time requirement instead. However, given the importance of maximizing the range in the case of electric aircraft, a cruise speed which enables high aero-propulsive efficiency is prioritized over a cruise speed which reduces block time.

In any case, given the relatively short range of electric aircraft, higher cruise Mach numbers would reduce the block time of the mission by several minutes at best.

The cruise altitude is treated as dependent variable, and computed to ensure cruise flight near maximum L/D. No constraints are included in terms of one-engine-inoperative (OEI) ceiling, since early analyses indicated that this would not be a limitation for electrically-driven propulsors without power lapse. Additionally, the AEO and OEI climb performance requirements of EASA CS-25 [16] are applied. Since it is currently unclear how regulations will evolve for such aircraft, "OEI" is treated here as the failure of just one of the N propellers of the aircraft, while the most restrictive value (corresponding to four-engine aircraft) is selected for climb-gradient requirements. Finally, to verify that the aircraft has enough power to climb after take-off, an AEO climb gradient of 8% at sea level is added to the performance constraints.

D. Operational Requirements

To compete effectively with narrowbody aircraft, several narrowbody-like constraints are imposed on the design. Firstly, the aircraft must fit in category C airport gates, i.e. the span must be below 36 m. To limit the turnaround time, a maximum battery charging time of 45 minutes is imposed. Note that this time is only necessary if the aircraft fully depleted its energy reserves in the previous mission. In most cases, the aircraft does not fly the harmonic mission, and therefore only part of the battery capacity has to be recharged. Thus, the average charging time is less than 45 mins. The battery system must be designed such that battery replacement can be performed during planned maintenance intervals in hangars with dedicated tooling. This allows for battery-pack designs with a higher degree of integration with the airframe, compared to swappable or line-replaceable units.

Due to the relatively short range of the aircraft, a web-like network of short routes would greatly enhance its decarbonization potential, as discussed in Sec. IV.D. In such a network, the aircraft would often operate from secondary airports (with a runway of at least 2000 m) and with frequent stopovers. This implies that several aspects of the aircraft, such as the cabin layout and luggage compartments, must be designed with stopovers in mind. These aspects are not discussed in further detail in this paper. However, both when operating from large international and secondary regional airports, noise is key for societal acceptance. Therefore, the aircraft should comply with ICAO Annex 16, Chapter 14 [17] limits, and ideally produce less noise than the latest-generation turboprop and turbofan aircraft. While no detailed noise assessment has been performed at this stage, several qualitative considerations are discussed in Sec. IV.E.

III. Conceptual Design of a Battery-Electric 90-Seater

To verify the parametric analyses of Part I [8], an electric aircraft is sized for the top-level aircraft requirements specified in Sec. II, using a Class-II design method. The basis of the method is described in Ref. [18], is validated in Ref. [19], and is expanded to account for the Class-II weight breakdown of Torenbeek [9] and the drag component buildup of Raymer [20]. The energy requirements for the battery and fuel are computed using a time-stepping mission analysis which accounts for climb, cruise, descent, diversion, and loiter. Assumptions regarding the efficiency and specific power of the powertrain components, take-off and landing performance modeling, energy consumption of non-propulsive systems, etc., are provided in Appendix A.

A. Key Design Choices

In the design-space exploration phase, several technologies (boundary-layer ingestion, ultra-high aspect-ratio wings, tip-mounted propellers, etc.) and configurations choices (high vs. low wing, V-tail vs. T-tail, 4 vs. 5 abreast, etc.) were evaluated. For brevity, only the main design choices leading to the final configuration are discussed here. Most of these design choices focus on minimizing the empty-mass fraction. Despite evaluating several radical technologies, the exploration phase converged towards a relatively conventional tube-and-wing design, as can be seen in Fig. 1. The main difference compared to conventional configurations becomes evident when comparing the proportions of the aircraft to a fuel-based counterpart. Figure 1 shows how the fuselage of the electric aircraft is significantly smaller than that of an A320, since it carries half the amount of passengers. However, the wing is significantly larger. In other words, the electric aircraft has a large wing relative to its fuselage—as explained by some of the scaling effects discussed in Part I [8]. In the following subsections, the design choices made for this aircraft are further elaborated.

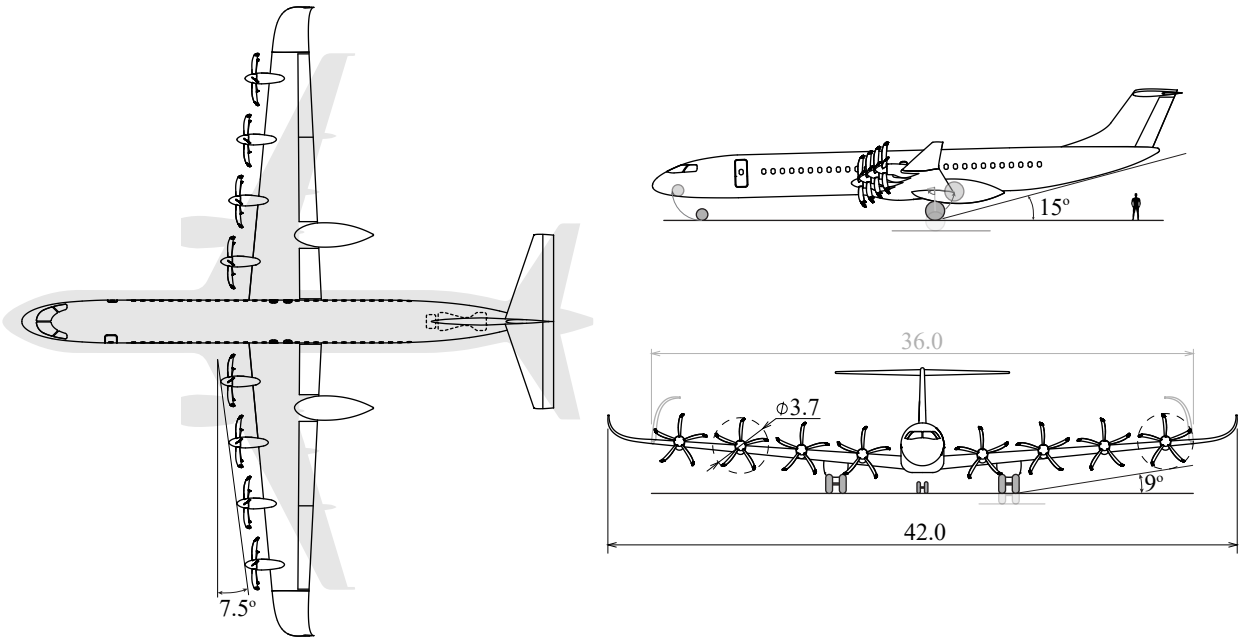

Fig. 1 Three-view of the 90-seater battery-electric aircraft. Top view includes A320 planform for scale in gray and the location of the reserve energy system, indicated with dotted lines.

1. Wing Design

The wing combines several characteristics to minimize the empty weight fraction of the aircraft:

- **Batteries in wing**: Placing the batteries in the wing is crucial to minimize the structural weight of the aircraft, since it reduces the root bending moment compared to having batteries in the fuselage, and thereby reduces the wing structural weight—assuming the wing structure is predominantly sized by the 2.5g pull-up maneuver, as is generally the case with commercial aircraft [21]. This design choice comes with its own challenge regarding access to batteries for replacement and ensuring safety in case of cell or module failure (e.g. thermal runaway*). This requires an integrated design of the battery-wing system where several compromises have to be made (*Challenge 1*). However, the substantial weight reduction enabled by placing batteries in the wing gives ample room for new integration solutions. For the design proposed in this paper, the battery pack occupies less than 50% of the volume of the wing box (i.e. the space available between the front and rear spars) if a pack-level mass density of 3000 kg/m3 is assumed. This provides room for a smart packaging of the batteries that facilitates inspection and replacement when necessary.
- **Low-wing configuration**: A low wing leads to a shorter, and thus lighter, main landing gear. The combination of multiple, smaller propellers and wing dihedral allows for a low wing while maintaining an acceptable ground clearance, as indicated in Fig. 1. A high wing configuration with batteries located in the wing is expected to be particularly heavy, since the fuselage would have to be reinforced to transmit loads to the landing gear (for fuselage-mounted landing gear) or absorb loads in case of a belly landing (for wing-mounted landing gear).
- **Modest aspect ratio**: generally, a high aspect ratio is targeted for electric aircraft, due to the importance of achieving a high lift-to-drag ratio (L/D) (see e.g. [23]). However, there are several reasons why a more modest aspect ratio is more beneficial in this case than for conventional aircraft. First, because a lower A implies a smaller wing span, making it easier to satisfy the airport span constraint. Second, because the wing volume scales with $V \propto S^{3/2}A^{-1/2}$, leaving more volume for batteries and other powertrain components inside the wing. And third, because a lower aspect ratio is expected to lead to less critical aeroelastic and landing loads, which is beneficial for wing structural weight. At this stage it is unclear if these load cases are strongly limiting for the wing structural weight (*Challenge 2*), since placing the batteries in the wing alleviates the 2.5g pull-up maneuver

*Note that for the battery to be certified in the first place, the module itself must prohibit failure propagation. See for example Ref. [22] and its list of references.

load but deteriorates the landing loads, compared to conventional aircraft. Based on these considerations, an aspect ratio of $A = 12$ is selected, similar to existing turboprop aircraft.

- **Folding wing tips**: even with a "modest" aspect ratio, the high maximum take-off mass (MTOM) combined with a low wing loading (Sec. III.A.6) leads to a large wingspan, which makes it challenging to fit within the gate span constraint while maintaining an acceptable aerodynamic performance. To circumvent this at the expense of a slight increase in wing weight, foldable wingtips are employed, similar to ones on the Boeing 777X.

2. Landing-Gear Placement

The main landing gear is installed behind the rear spar and is retracted rearwards into the pods visible in Fig. 1. There are two main reasons why a wing-mounted landing gear is preferred over a fuselage-mounted gear. First, since it is placed further outboard, a shorter gear is needed to satisfy the propeller ground clearance constraint in case of a banked landing. Second, it minimizes bending moments in the wing during landing or a taxi bump. This configuration also comes with drawbacks, such as reduced space for trailing-edge high-lift devices, or a larger turn radius on the ground. The landing-gear pod also contributes to weight and friction drag. However, the alternative fuselage-mounted gear would also require a large fairing: since the fuselage is relatively small (driven by payload weight) and the gear is relatively large (driven by max landing weight), it is impossible to store the main gear inside the fuselage itself.

3. Propulsion System Integration

The number of propellers is determined in a trade-off between disk loading, propeller noise, landing gear length, OEI power requirements, motor rotational speed, nacelle drag, and slipstream effects on wing performance. This leads to a configuration with eight propellers covering the full available wing span, while maintaining sufficient clearance between propellers to limit interaction noise, which decreases rapidly as the separation between adjacent propellers is reduced [24]. The resulting low disk loading (377 N/m² in cruise, compared to typical twin-turboprop values of $500 - 800$ N/m²) ensures a high propeller efficiency in cruise and, especially, during take-off. The latter is particularly important due to its impact on the required motor power in the sizing condition. Moreover, while some studies suggest that using a gearbox is lighter than a direct-drive solution [25], we initially opt for a direct-drive arrangement to reduce the complexity of the system. This implies that the electric motors have to operate at low rotational speeds, in the order of 800 to 1400 rpm.

4. Reserve Energy System

A gas-turbine-based turbogenerator is located in the tail cone to provide power to the batteries and motors in the case of diversion or loiter. The term "range extender" is avoided here, since the primary purpose of the reserve energy system is to cover reserves, and not enhance mission range. For the same reason, the aircraft is described as "battery electric", although technically it is a serial hybrid architecture. Note that the turbogenerator could in fact be used as "range extender" without major changes to the aircraft but, in that case, the emissions and operating costs of the aircraft are found to increase. Several decisions remain regarding the design of the reserve energy system (*Challenge 3*). For example, it is undecided whether for the envisioned application, two gas turbines would be required for redundancy. Although that would have a substantial impact on aircraft weight and costs, it remains a much lighter solution than to use the batteries to cover reserves [8]. In this paper, a single turbogenerator is assumed.

5. Tail Configuration & Fuselage Cross Section

The required horizontal-tail surface area scales with $1/l$, with l being the distance between the aerodynamic center of the wing and the aerodynamic center of the tailplane. Since the electric aircraft has a large wing relative to the fuselage, the tail is closer to the wing (in a non-dimensional sense) than in conventional aircraft. Therefore, to minimize horizontal tail size—and thus, drag—a T-tail configuration with a swept vertical tail is selected. During the design-space exploration phase, the choice for a 4-abreast arrangement (heavier fuselage) over a 5-abreast arrangement (lighter fuselage) was also primarily driven by the reduction in tail size enabled by the more slender fuselage. A T-tail configuration also ensures that the propeller slipstreams do not impinge on the horizontal tail at low to moderate angles of attack, although additional analyses are required to assess the impact at high angles of attack and mitigate deep stall.

6. Wing & Power Loading

Figure 2 shows the wing/power loading diagram of the aircraft. The area in gray indicates the combinations of wing loading (i.e. wing size) and power loading (i.e. powertrain size) which satisfy all performance requirements. Assuming a maximum lift coefficient of $C_{L\max} = 2.5$, the landing distance required is met with a wing loading of approximately 5 kN/m². This modest $C_{L\max}$ is lower than typical narrowbody aircraft, and may be attainable with a plain flap with propeller slipstream effects, though that raises the question whether future regulations will be adapted to allow determination of the stall speed in power-on conditions, in the case of distributed-propulsion aircraft. The $C_{L\max}$ can also be increased using more complex high-lift devices, but this is counterproductive: when evaluating the design at higher wing loadings, the MTOM increases. Previous studies [12] have already shown that this occurs because the take-off requirement is the active constraint, and therefore a higher wing loading leads to a lower power loading and, subsequently, a higher powertrain weight. This is contrary to other electric aircraft design studies which attempt to use distributed propulsion to maximize the wing loading (see e.g. Ref. [23]). On the other hand, an excessively low wing loading leads to a large wing, which in turn makes it difficult to satisfy the maximum span constraint. In this study, we assume a maximum folding wingtip span of 3 m per side to ensure that the ailerons, which are located inboard of the folding location, retain sufficient control authority (for context, note that the Boeing 777X has folding wingtips of 3.5 m length). Further research is required to determine whether larger or smaller folding wingtips are possible. With this assumption and the gate span constraint of 36 m, the maximum wingspan of the aircraft can be 42 m.

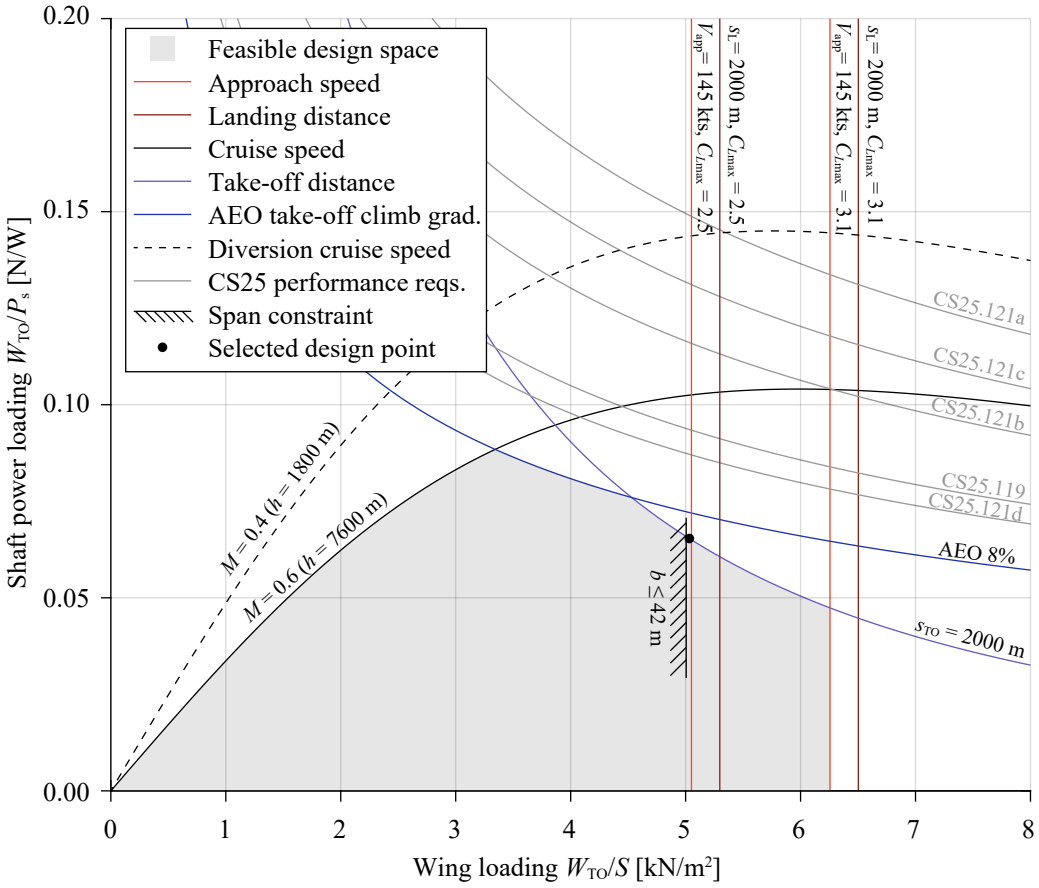

Fig. 2 Wing-loading/power-loading diagram of the battery-electric aircraft. The power values refer to the maximum continuous shaft power of the electric motors.

Based on these considerations, the wing loading of approximately 5 kN/m² is selected as design point. At this wing loading, the power loading is determined by the take-off constraint, while the cruise speed constraint can be met with much higher W_{TO}/P_s values. The difference between take-off power and cruise power implies that the cruise speed can be increased beyond $M = 0.6$ without imposing any penalty on powertrain weight. While some high-speed propeller designs have shown constant efficiencies up to a cruise Mach number of 0.75 [26], a more detailed analysis

of the propeller and wing aerodynamics is required to determine how much the Mach number can be increased with deteriorating the aero-propulsive efficiency of the aircraft, $\eta_p(L/D)$.

B. Sizing Results

The resulting mass breakdown of the aircraft is shown in Fig. 3. If we consider the fuel of the reserve energy system as part of the empty mass for bookkeeping purposes, we see that an empty-mass fraction of 42% is obtained, including the reserve energy system. This is in line with the Class-I analyses of Part I [8]. The figure also indicates a battery mass fraction of 46%. Placing 46% of the aircraft mass inside the wing is highly unusual for turboprop aircraft, but energy fractions of around 45% are not unheard of for jet aircraft—see e.g. the Boeing 707-320 or DC-8-63.

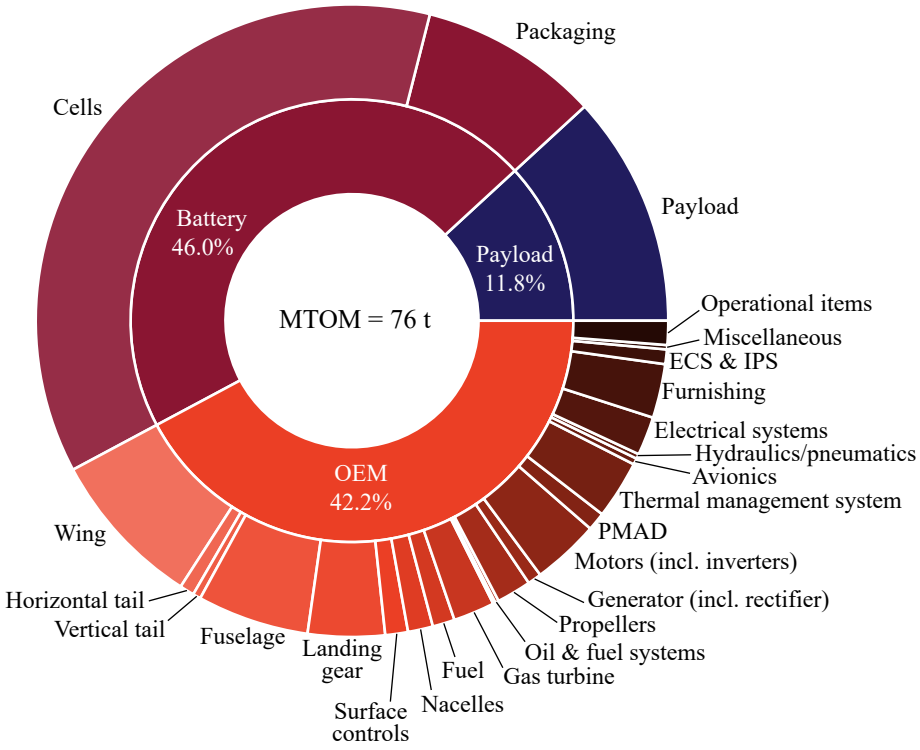

Fig. 3 Class-I (inner circle) and Class-II (outer circle) mass breakdown of the 90-seater battery-electric aircraft at maximum take-off mass. Note that for bookkeeping purposes, the OEM includes fuel mass of the reserve-energy system.

Although these results are encouraging, there are also several uncertainties which require further verification. For example, the wing structural mass is computed using handbook methods [9], which are partially based on statistical data. The question is whether such correlations remain accurate in a configuration where different load cases may be driving the structural mass (*Challenge 2*). Analogously, there is uncertainty regarding the masses of the high-voltage (*Challenge 4*) and thermal management system (*Challenge 5*) components of the powertrain, which are estimated using simple assumptions for power density based on literature (see Appendix A). The same applies for non-propulsive systems such as the flight control system (FCS), ice protection system (IPS), or environmental control system (ECS), for which an increased degree of electrification may lead to different architectural choices and weights, compared to conventional aircraft (*Challenge 6*). More detailed investigations are required to confirm the accuracy of these assumptions. And finally, there is uncertainty in the assumptions made with respect to battery cells and packaging. These characteristics have a large impact on MTOM and are discussed in the following section.

To illustrate how scaling effects in electric aircraft influence the lift-to-drag ratio, Fig. 4 compares the drag breakdown of the electric aircraft to a fuel-based turboprop reference aircraft designed with the same tool for the same mission, in cruise conditions. The figure shows how the lower fuselage drag coefficient is the main reason for lower drag coefficient in the electric aircraft. A slightly lower induced drag coefficient is also achieved, due to the higher Oswald factor (less

fuselage disturbance on the wing). Overall, this leads to a relatively high lift-to-drag ratio of $L/D = 23$. However, also here there are some uncertainties. For example, the drag due to heat exchangers cannot be accurately modeled at this stage (*Challenge 5*), and a more detailed control & stability analysis is required to calculate the required tail area for this distributed-propulsion aircraft (*Challenge 7*). Moreover, the effect of the propellers and—especially—the nacelles on wing performance must be assessed in more detail. This has been investigated to a certain extent in previous studies [27], but is especially critical for high-lift performance (*Challenge 8*). In any case, the resulting lift-to-drag ratio is significantly higher than the fuel-based counterpart.

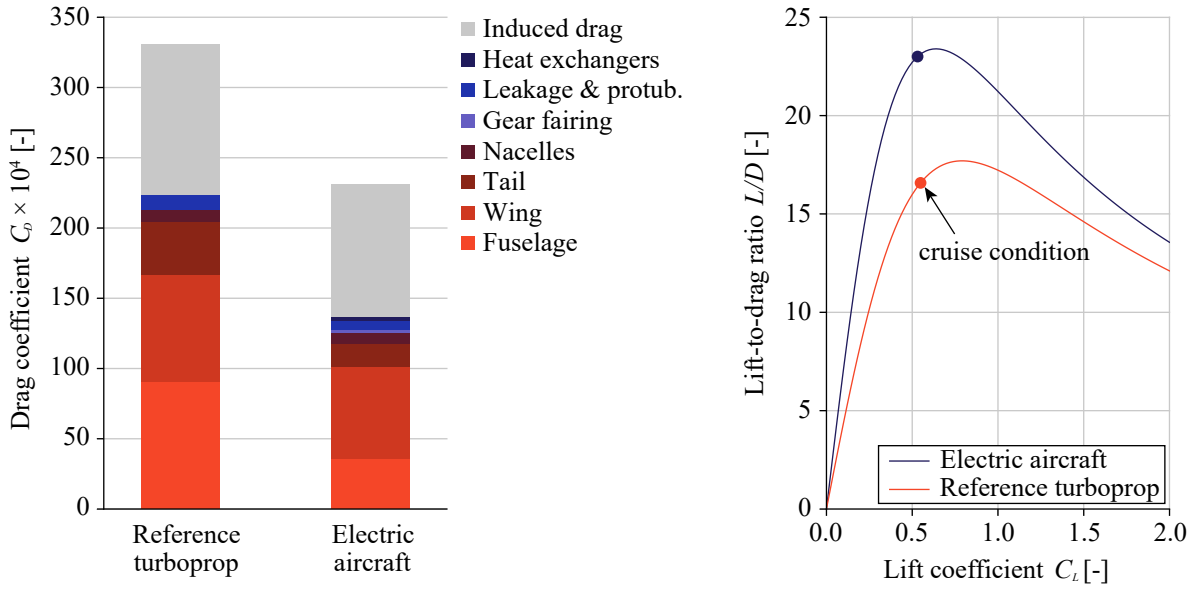

a) Drag breakdown in cruise **b) Lift-to-drag ratio polars**

Fig. 4 Drag breakdown and lift-to-drag ratio of the battery-electric aircraft compared to a conventional twin-turboprop reference configuration, designed for the same mission. Propeller interaction effects neglected.

To summarize, Table 2 presents an overview of some of the main characteristics of the aircraft. Note the high estimated propeller efficiency as a result of the low disk loading.

Table 2 Overview of main design results. The quoted empty-mass fraction, OEM/MTOM, includes the mass of the reserve energy system (i.e. gas turbine, generator, fuel, and accessories).

Parameter	Value	Parameter	Value
MTOM [t]	76.0	L/D (cruise)	23.0
OEM/MTOM	42%	Max cont. power per motor [MW]	1.4
BM/MTOM	46%	Propeller efficiency (cruise)	0.87
PLM/MTOM	12%	Propeller diameter [m]	3.7

C. Range Versus Battery Technology Scenarios

The achievable range depends on the battery energy density, and the achievable energy density depends on other characteristics of the battery. In this study, we make the following assumptions:

- A maximum (dis)charge rate of **1.35C** stems from the top-level aircraft requirement of 45 mins charging time. Since the aircraft carries a significant amount of energy in the batteries—of the order of 11 MWh—the peak discharge rate during take-off is relatively low (~1.3C). These C-rate requirements are substantially lower than those of ground-based vehicles and eVTOL aircraft [28].

- A packaging is required to connect, manage, and ensure the structural integrity and safety of the cells. We assume a **25% packaging mass overhead** (i.e. a cell-to-pack ratio of 0.8). This target is aligned with the targets established in several roadmaps [29] and eVTOL manufacturers have been said to achieve overheads below 25%, though the question is whether this is also achievable with higher-energy-density cells [30]. For this 25% overhead, a smart integration solution of the battery pack on the aircraft is required, with airframe elements potentially contributing to structural, thermal, or other safety functions of the pack (*Challenge 1*).
- The battery has a **maximum depth-of-discharge of 90%**, as suggested by Ref. [31]. In other words, the state-of-charge can vary from approximately 95% to 5%. Note that this maximum discharge is only required on very limited occasions, when the aircraft flies its maximum range and is additionally required to perform a go-around.
- An end-of-life capacity of 90%, i.e. the battery is replaced after **10% capacity degradation**. Although this is important for sizing the thermal management system, it is more of an operational choice than an assumption. Retiring the battery "ahead of time" is required to maintain range capabilities. However, an operator that only flies short routes may opt to retire the battery pack after >20% degradation in order to extract more cycles.
- Battery cycle life is an important driver for operating costs and environmental impact. In our calculations, we assume the battery is replaced after **1500 cycles**. However, we must realize that an aircraft does not always fly the design range, but a distribution of ranges instead. For the distribution of flights provided to this study by a major international airline, roughly 30% of flights (i.e., only 450 cycles) would correspond to "deep" discharges above 70% DoD. These assumptions imply that the battery pack has to be replaced once or twice per year, depending on the usage of the aircraft. This should be seen as a planned base maintenance operation, and not a line maintenance activity.

The resulting relation between the energy density of a new cell and the useful, end-of-life pack energy density is shown in Fig. 5.

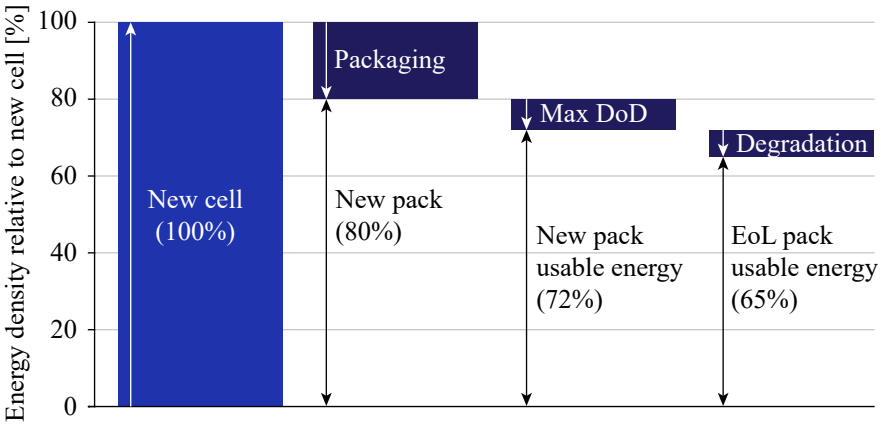

Fig. 5 Battery energy-density waterfall chart.

With the packaging overhead and other characteristics of the battery specified, we define three cell energy-density scenarios in Table 3: a conservative scenario of 300 Wh/kg (corresponding to current state-of-the-art cell technology), a baseline scenario of 450 Wh/kg for a 1st generation aircraft, and a future scenario of 550 Wh/kg for a 2nd generation aircraft (which would be required to achieve the targeted 1000 km range). Note that the cells must be able to provide these energy densities at the C-rates quoted above; if not, an additional knock-down factor must be considered [32].

The aircraft achieves ranges of 500 km, 800 km, and 1000 km for cell energy densities of 300 Wh/kg, 450 Wh/kg, and 550 Wh/kg, respectively. This is shown in Table 3, where the range values refer to the useful air range, which takes into account the energy required for taxi, take-off, reserves, power off-takes, etc. While the 450 Wh/kg and 550 Wh/kg cases require further cell technology development, they are much less aggressive requirements than the *pack-level* 500 to 1000+ Wh/kg that literature suggests is necessary to make an electric passenger aircraft viable [5, 28, 31, 33]. The development of cells with these energy densities and the other performance metrics listed above is one of the key drivers to further enhance electric aircraft range (*Challenge 9*).

Table 3 Useful air range obtained for various 2030+ battery technology scenarios. Ranges are quoted at approximately 3% cell capacity degradation (i.e. one-third into the useful life on the aircraft).

	Conservative	1st gen aircraft	2nd gen aircraft
Cell energy density [Wh/kg]	300	450	550
Pack energy density [Wh/kg]	240	360	440
Ramge [km]	500	800	1000

IV. Environmental Assessment

A. Alternative Energy Sources for Aircraft Propulsion

Three main energy carriers are generally considered for a future "zero-emission" air transport system: batteries, hydrogen, and sustainable aviation fuel (SAF) [1]. For a fair environmental assessment of electric aircraft, they should not only be compared to current kerosene-based aircraft, but also to other aircraft with new technologies that may appear in the coming decades. For this comparison, we assume that hydrogen is used in liquid form, which offers a higher volumetric density than gaseous hydrogen and is considered more beneficial for passenger transport aircraft [6]. Among the different types of SAF, here the comparison is performed with power-to-liquid synthetic fuels ("eSAF") including direct air capture, which—to the best of our knowledge—is the only SAF pathway to achieve a net-zero-CO_2-emission energy carrier that can be scaled up to power the complete aviation sector in the future. While other types of SAF such as biofuels are also beneficial for emissions, they are an unlikely candidate for decarbonization of the aviation sector as a whole due to challenges associated with scaling up production to satisfy the demand in a sustainable manner [1, 34].

In this analysis, electricity can be used to produce eSAF, charge batteries, or produce liquid hydrogen for direct combustion or use in a fuel cell. For an apples-to-apples comparison, these four pathways use electricity from the same grid†. For zero CO_2 emissions, this electricity has to be produced with renewable ("green") electricity. However, most energy produced around the world today comes from non-renewable sources. Assuming that 100% green electricity can be used for battery, eSAF, or hydrogen-powered aircraft in a world where the electrical grid is not 100% renewable, and implying that other industries must use the non-renewable part, is a misleading argument. Therefore, instead, in Sec. IV.C we will analyze how different grid cleanliness-scenarios affect the comparison.

Figure 6 shows typical efficiencies associated with the various steps of the four pathways to bring electricity from the grid to the shaft of propulsor, based on discussions with experts and values encountered in literature [6, 34, 35]. The figure shows that, for a battery-powered aircraft, roughly 1.3 kWh of grid energy is required per kWh of energy at the shaft. For the hydrogen propulsion options, roughly 4 kWh of grid energy is required per kWh of shaft energy, and for eSAF this increases up to 5−9 kWh. In other words, bringing electricity directly to shaft is roughly three to six times more efficient than using hydrogen or eSAF, in terms of grid energy required per unit energy at the shaft. The following sections discuss how these ratios translate into differences in energy consumption and emissions.

B. Tank and Grid Energy Consumption

As reflected on the right-hand side of Fig. 6, the powertrain efficiency of a battery-electric aircraft is high compared to fuel-based aircraft, but a battery-electric aircraft is also very heavy on a per-passenger basis (low payload mass fraction; see Sec. III.B). Therefore, a priori it is not clear whether the aircraft is energy-efficient on a per-passenger-kilometer basis. To dive into this and illustrate the importance of accounting for the various pathway efficiencies, in this section we compare the energy consumption per passenger-kilometer of different modes of transport, for a mission range of the "1st gen" electric aircraft of 800 km. We compare the aircraft to existing modes of transport (narrowbodies, cars, and the train), and to hypothetical future competitors of the aircraft (hydrogen aircraft and a next-gen turboprop design). While these different forms of transport are designed for different ranges, here we are interested in how they perform on ranges where the electric aircraft may be an alternative. More specifically, we compare:

†One could argue that hydrogen or eSAF can be produced in a part of the world with abundance of renewable energy, and then transported to other parts of the world. However, in that case the energy (and costs) required for that transport must be included in the analysis.

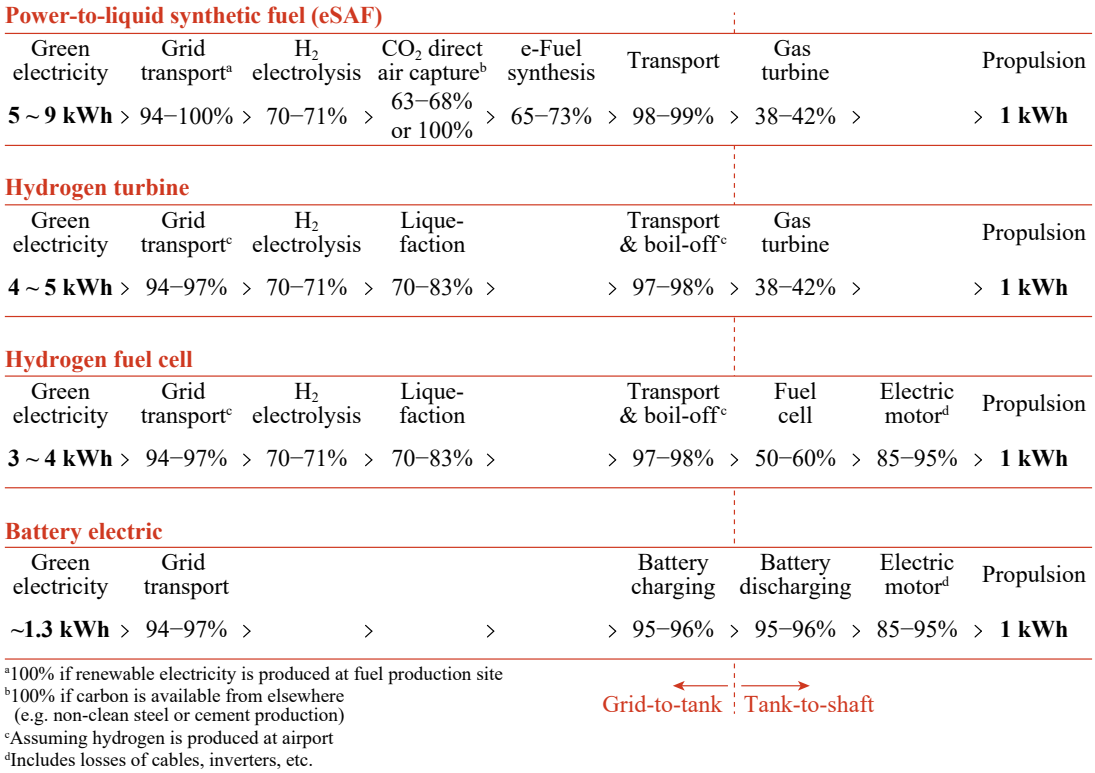

Fig. 6 Conversion efficiency of four pathways to bring renewable energy to the propeller shaft: eSAF, H_2 turbine, H_2 fuel cell, and battery electric.

- The "1st gen" electric 90-seater designed in this study, with a harmonic range of 800 km.
- A hypothetical next-gen, fuel-based, twin-turboprop reference aircraft designed for the same payload (90 passengers), range (800 km), and entry-into-service as the electric aircraft, to demonstrate the effect of battery-electric propulsion technology while keeping the requirements constant. This is the "apples to apples" comparison from a technical perspective.
- An A320neo-like narrowbody, which can carry around 180 passengers up to 6500 km. While this aircraft is designed for much longer ranges and therefore has a suboptimal energy consumption on such a short range, it is still the most commonly used type of aircraft for these ranges due to economic and operational reasons (see Sec. IV.D). Therefore, this would be the relevant comparison from a business-case perspective.
- A hydrogen fuel-cell regional aircraft concept of the Aerospace Technology Institute (ATI) [36], designed to carry 75 passengers a distance of roughly 1500 km.
- A hydrogen gas-turbine powered narrowbody aircraft concept designed by the ATI [36], designed to carry 180 passengers a distance of roughly 4500 km.
- A ground-based electric vehicle (EV, i.e. a car).
- An electrically-driven train operating on a densely traveled network.

For the ground-based modes of transport, stops or stopovers may be required to complete a 800 km mission, but here we focus the discussion exclusively on energy consumption per passenger-kilometer, which we assume to be independent of range for the car and train. For a fair comparison, we correct the energy consumption of all modes of transport for the average occupancy (85% load factor on planes, 1.2 passengers in a car, and the data of the train already accounts for this). The full list of assumptions can be found in Appendix B. The resulting energy consumptions per passenger-kilometer are shown in Fig. 7 in terms of vehicle (i.e. tank-to-wake) and grid (i.e. well-to-wake) energy consumption. Note that for the fuel-based aircraft we assess both Jet A1 and eSAF as alternatives, which becomes relevant in the next section.

Figure 7 illustrates that the battery-electric (167 Wh/pax-km) and conventional propeller (187 Wh/pax-km) aircraft designed for 800 km range are comparable in terms of vehicular energy consumption per passenger kilometer, shown in dark blue. While the electric aircraft (76 t) is more than twice as heavy as the reference turboprop (28 t), this

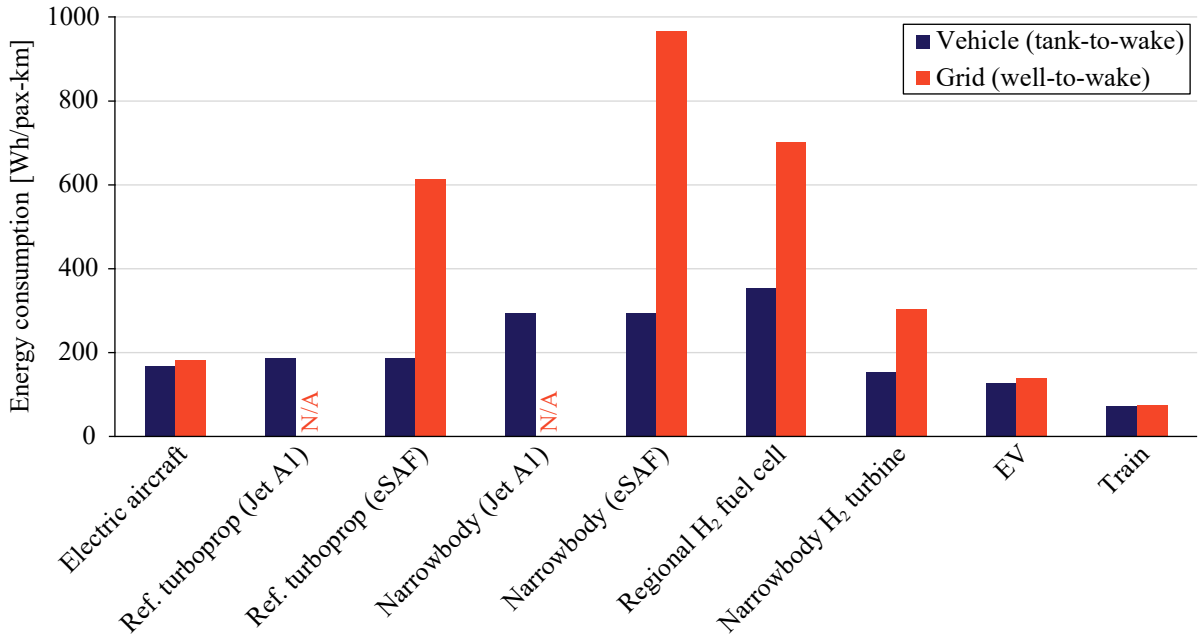

Fig. 7 Comparison of vehicle and grid energy consumption per passenger-kilometer for various aircraft configurations and land-based modes of transport. Comparison performed for a mission range of 800 km.

is compensated by a much higher powertrain efficiency and slightly higher lift-to-drag ratio. Both aircraft have a substantially lower energy consumption per passenger kilometer than the narrowbody at these ranges. The figure also shows that vehicle energy consumption of the electric aircraft is in the same ballpark as the H_2 narrowbody and an electric car, on a per-passenger-kilometer basis. In this comparison and based on the values reported in Ref. [36], the H_2 narrowbody has a substantially lower tank energy consumption than the fuel-based narrowbody and the H_2 fuel cell, though the reason for this is unclear.

However, the vehicle energy consumption per passenger kilometer at tank level is neither representative of the energy costs nor of the life-cycle emissions. For that, the energy required from the grid to produce the energy used on the aircraft is more representative. This is also shown in Fig. 7 and is obtained by multiplying the tank energy consumption per passenger kilometer by the average grid-to-tank conversion efficiency shown in Fig. 6. The graph shows that the battery-electric aircraft requires approximately 70% and 80% less grid energy per passenger kilometer than the eSAF-based regional and narrowbody aircraft, respectively. Compared to the hydrogen-based aircraft, the reductions are approximately 75% and 40% for the regional (fuel cell) and narrowbody (turbine) configurations, respectively. The energy consumption of the electric aircraft remains comparable to the ground-based electric vehicle and is roughly twice as high as the train, on a per-passenger-kilometer basis. These numbers suggest that in terms of both environmental impact and energy costs, the electric aircraft is a highly efficient mode of transport.

C. Comparison of Emissions

Now that we know the tank and grid energy consumptions per passenger kilometer of the different vehicles, we can make a preliminary assessment of their environmental impact. Accurately quantifying the environmental impact is very challenging and thus here we perform only a simplified analysis, the assumptions of which can be found in Appendix B. While this analysis only gives a first indication of the environmental impact of the various modes of transport, the stark differences between the different options are larger than the uncertainty bands and allow for meaningful conclusions. For this simplified analysis, we use the well-to-wake "CO_2-equivalent" per passenger-kilometer as an indicator of the impact on global warming. In this CO_2-equivalent we account for emissions produced during the mission, emissions generated in the production of the energy consumed during the mission, and emissions produced in the manufacturing of batteries. Emissions generated in the manufacturing process of the vehicle or the infrastructure are not included in this analysis. For in-flight emissions, we consider both CO_2 and non-CO_2 effects, which can be significant [37]. Since there is significant uncertainty regarding several of these assumptions, the results are presented in Fig. 8 with conservative error bars that give a notional indication of the possible error band.

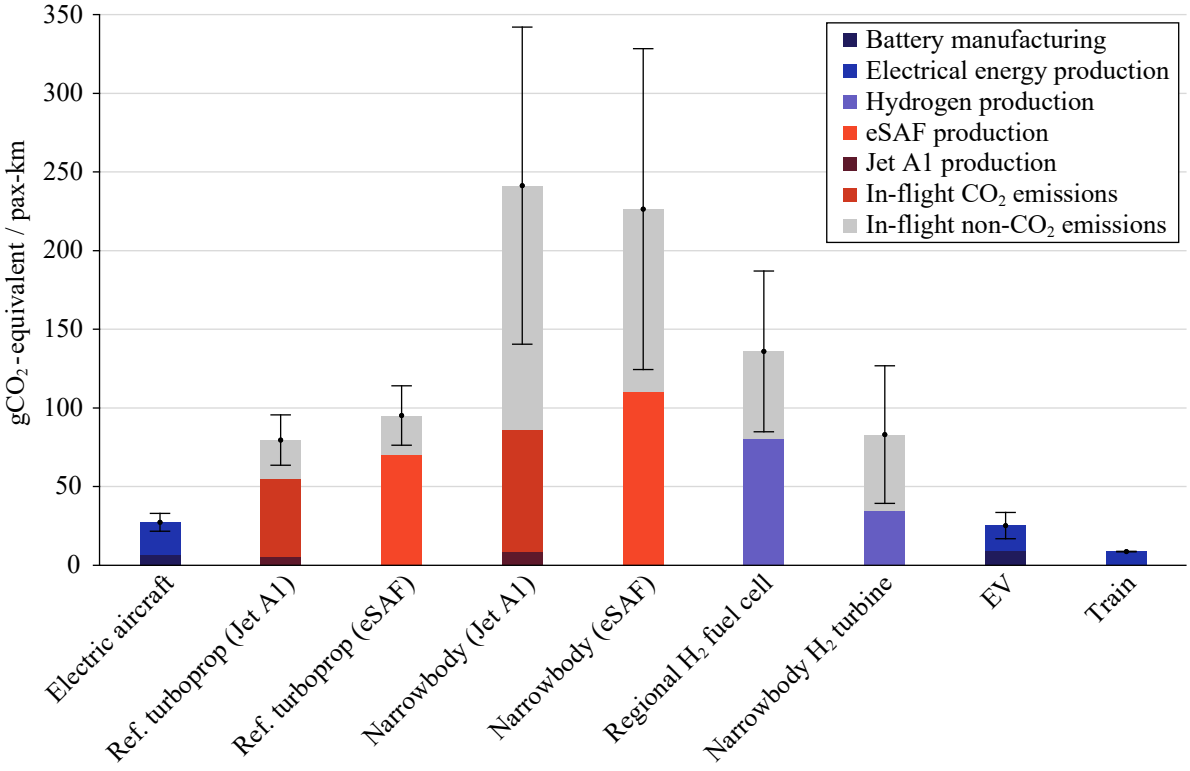

Fig. 8 Breakdown of equivalent CO_2 emissions per passenger-kilometer, for various aircraft configurations and land-based modes of transport. Results presented for a "clean" EU 2030 target grid emission index of 114 gCO_2/kWh. Comparison performed for a mission range of 800 km.

The emissions presented in Fig. 8 correspond to a grid with an emission index of 114 gCO_2/kWh, which is targeted for 2030 in Europe [38]. This emission index is representative of a grid with a high degree of renewables, and is comparable to e.g. Denmark in 2019 [39]. For the conventional turboprop and narrowbody, both eSAF and kerosene (Jet A1) options are included. The figure shows how, for electric vehicles, the contribution of battery manufacturing to total lifecycle emissions is smaller than the contribution of the electrical energy consumed during operation. The figure also shows how, for the selected grid emission index, eSAF is not necessarily better than kerosene for conventional aircraft. Moreover, the hydrogen aircraft present higher CO_2-equivalent emissions than the advanced turboprop. This is partially due to increased non-CO_2 effects and a relatively heavier aircraft (additional mass due to e.g. the hydrogen tank and the airframe mass required to accommodate it), but also partially because, like the fuel-based narrowbody, they are over-sized for an average trip length of 800 km.

Two important conclusions can be drawn from Fig. 8. First, despite the significant uncertainties, the battery-electric configuration presents a clear advantage over the other aircraft configuration in terms of CO_2-equivalent/pax-km. In other words, "if the mission *can* be flown electrically, then it *should* be flown electrically". From this perspective, kerosene, hydrogen, or eSAF should only be used for higher ranges that are not achievable with battery-electric propulsion. And second, if we compare the battery-electric aircraft to the car and train, we see that these lie in the same ballpark in terms of CO_2-equivalent per passenger-kilometer. However, this does not consider infrastructure requirements, such as the impact of railway and road construction and maintenance on emissions and land use, nor the fact that cars and trains generally travel in a less straight line from origin to destination. This suggests that such an aircraft is comparable to electric land-based modes of transport from an environmental perspective. It also implies that bans on flights for short distances, such as the ban imposed in France [40], are unnecessary for a battery-electric aircraft.

The aforementioned conclusions are valid for the selected "EU 2030" grid scenario. However, on one hand the current world grid uses much less renewable energy, and on the other, we strive to obtain a fully renewable grid in the future. So, what does the comparison look like in those scenarios? For this, Fig. 9 shows the CO_2-equivalent emissions of the various modes of transport for the 2019 world average emission index (475 gCO_2/kWh [41]), the EU 2030 target

(114 gCO_2/kWh; used in the previous figure), and a hypothetical fully-renewable grid (0 gCO_2/kWh). Note how the Jet A1 aircraft are slightly affected by the grid scenario due to the fuel production phase. The figure shows that, with the 2019 electricity mix, the electric 90-seater is comparable to a next-gen turboprop designed for the same mission, but already presents less CO_2-equivalent emissions than a latest-generation narrowbody or hydrogen-based alternatives.

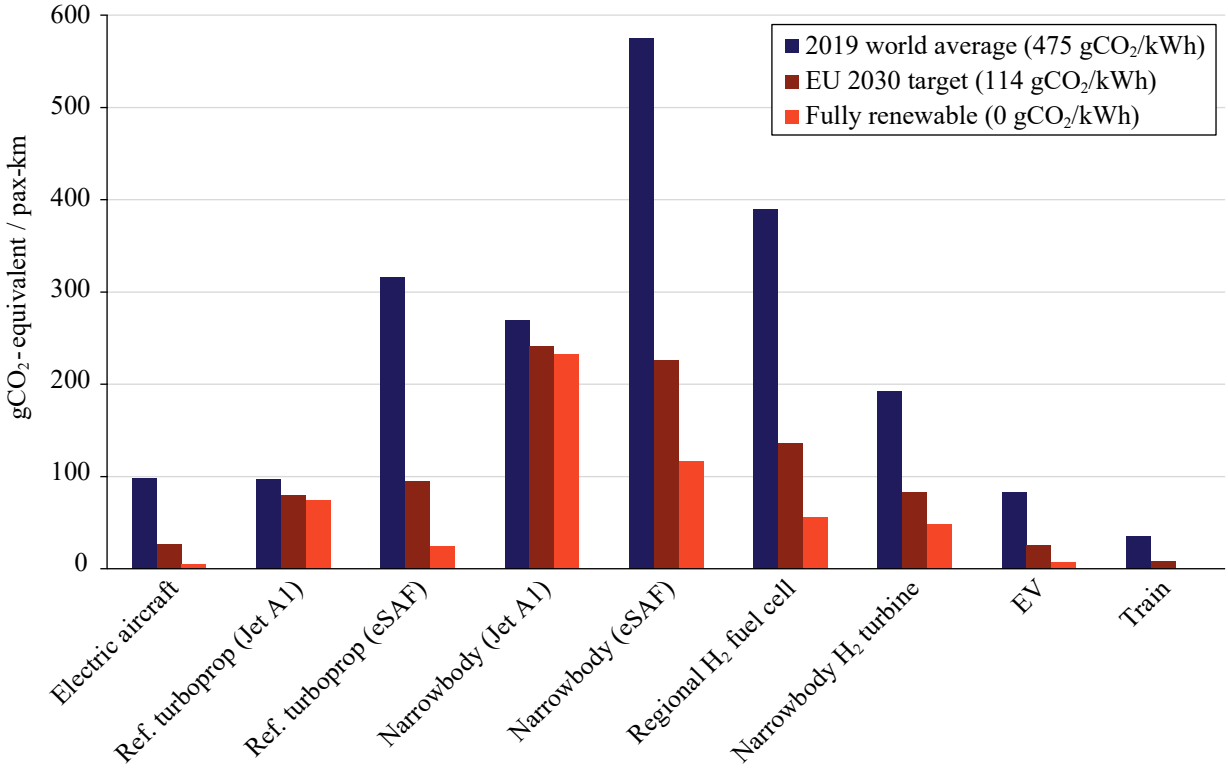

Fig. 9 Comparison of equivalent CO_2 emissions for various grid cleanliness scenarios. Errorbars are omitted to improve readability; see Fig. 8 for an indication of the uncertainty.

Another relevant takeaway from Fig. 9 is what the authors refer to as the "SAF paradox": while SAF is generally seen as a short-term solution because the technology is relatively easy to implement, it only becomes a scalable sustainable solution on the long term, when the grid is (almost) completely renewable. On the short term, it is either not scalable (biofuel), or not sustainable (synthetic fuel). Although the use of biofuels does help to reduce global warming and should therefore be encouraged as much as possible, the overall "decarbonization" potential of SAF will remain limited until there is an abundance of green energy. Until then, the development of battery-electric and hydrogen technologies is key to reduce emissions. In fact, an extensive use of battery-electric propulsion for short ranges would allow us to save a scarce H_2 or SAF supply for longer-range missions.

D. Potential Impact on Aviation Sector

Figure 8 shows that the electric aircraft produces approximately 90% lower CO_2-equivalent emissions than the latest-generation narrowbody flying on Jet A1, for the EU 2030 grid cleanliness scenario. This reduction increases to nearly 100% if the grid becomes fully renewable. Since the Airbus A320neo and Boeing 737MAX are currently the latest-generation narrowbodies, we consider their emissions (be it due to the combustion of kerosene or the production of SAF) to be representative of the average narrowbody fleet emissions in the 2030+ timeframe, as they will gradually replace existing older aircraft models. However, these aircraft—and especially widebody aircraft—have substantially higher design ranges than the electric aircraft. This raises the question whether electric aircraft, despite the potential emissions reduction of over 90% on a per-passenger-kilometer basis, will have a significant effect on the aviation sector as a whole, or whether the effect is negligible due to the relatively short ranges to which they are limited.

To put this into perspective, Fig. 10 shows the distribution of CO_2 emissions produced by commercial passenger transport, for different mission ranges. Note that this figure excludes non-CO_2 and other life-cycle emissions. The data

shown in this figure corresponds to the year 2019, prior to the COVID-19 pandemic. While most studies agree that the amount of passenger-kilometers flown globally will increase substantially in the coming decades (for context: several studies suggest that the amount of passenger-kilometers will roughly triple by 2050, relative to 2020 [42]), in this simple analysis we assume that the distribution of flights in the 2030+ timeframe will be comparable to the one shown in Fig. 10. Looking at this distribution and focusing on regional flights below 2000 km, we can draw two important conclusions. First, we see that these ranges are dominated by narrowbody aircraft, and not by regional aircraft. The narrowbody aircraft emit less CO_2 on a per-passenger-kilometer basis than regional aircraft [7] due to the higher seat count, and therefore their share of passenger-kilometers is even higher than the bars suggest. And second, the figure shows that a significant portion of the total CO_2 emissions of the aviation sector are generated on ranges below 2000 km. In other words, while the contribution of *regional aircraft* to overall CO_2 emissions is relatively low, the contribution of the *regional market* to the overall CO_2 emissions is relatively large. And to assess the overall decarbonization potential of electric aircraft we must not focus on the regional aircraft, but on the regional market.

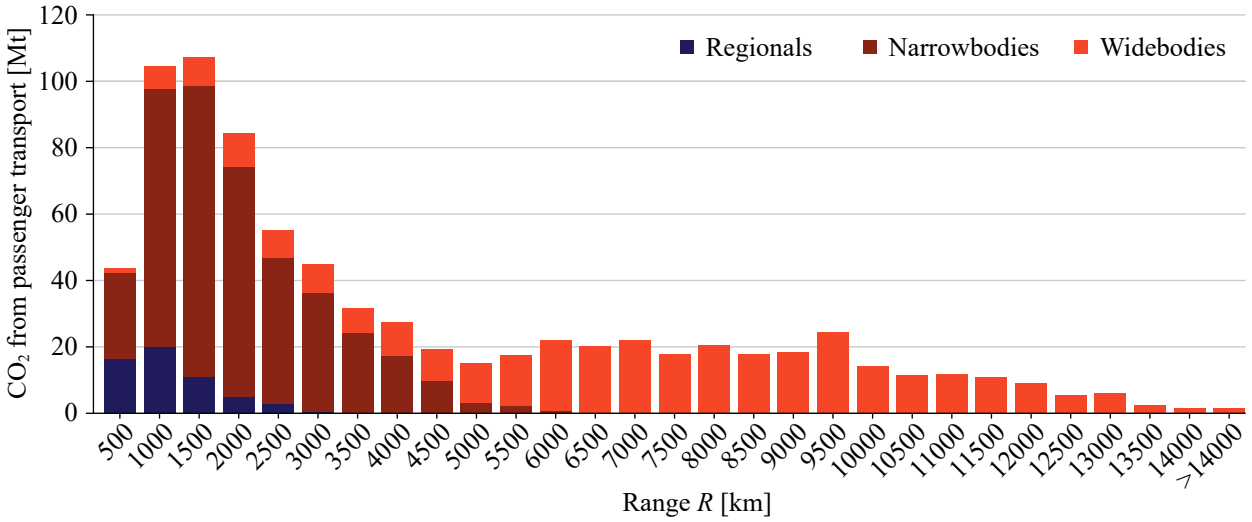

Fig. 10 Distribution of CO_2 emissions due to commercial passenger transport versus flight distance and aircraft type, in 2019. Adapted from Ref. [7].

To be more specific, Table 4 shows the share of CO_2 emissions and number of flights corresponding to ranges below 500 km, 800 km, 1000 km, and 2000 km. The number of flights is relevant not only for the market size, but also for the LTO emissions (landing and take-off cycle emissions, such as NO_x and soot) and noise produced in the vicinity of airports. If a battery-electric aircraft replaces a share of these flights, the associated LTO emissions are reduced to zero and the noise per flight may be reduced (see Sec. IV.E); however, note that a single narrowbody would have to be replaced by roughly two electric 90-seaters to transport the same volume of passengers, and therefore the required number of flights for short distances would increase noticeably.

The first three columns of Table 4 correspond to the ranges achievable with the electric aircraft for the three battery-technology scenarios collected in Table 3, while the fourth corresponds to the range a 1000 km electric aircraft could cover with one stopover. Although an effective use of stopovers would require a shift from a traditional point-to-point or hub-and-spoke network of operations to a more "web" based network where a fleet of aircraft operates from not only primary but also secondary airports (with 2000 m runway), the development of a zero-emission 90-seater would provide an opportunity to take advantage of currently under-served regional airports. This may allow passengers to cover 2000 km with a single stopover without noticeably increasing the overall door-to-door travel time, if the airports are closer to their original departure location and final destination. This line of thought has some parallels with the concept of Regional Air Mobility (RAM) [43], though further research is encouraged to investigate advantages and drawbacks of such operations in terms of economics and passenger experience.

In any case, Table 4 shows that, independently of the range scenario, the decarbonization potential of large electric aircraft is substantial. Note that the values do not consider non-CO_2 effects such as contrails, which are more difficult to quantify and are higher for longer-distance flights. The values of Table 4 also reflect a non-linear increase in emissions with range: the share of CO_2 emissions for 1000 km (19%) is more than double the share corresponding to 500 km (6%),

and the share corresponding to 2000 km (43%) is in turn more than double the share corresponding to 1000 km. This occurs because the 1000 km − 1500 km interval is the largest contributor (see Fig. 10), and reconfirms the importance of maximizing electric aircraft range to maximize their market potential. For example, a "1st gen" 90-seater with 800 km range has the potential to replace 41% of all flights and thereby reduce the CO_2 of the entire aviation industry by 14%, while the use of a "2nd gen" aircraft with 1000 km range and stopovers would increase these shares to 82% of all flights and 43% of all CO_2 emissions. These numbers evidence that, to truly maximize the decarbonization potential of this new propulsion technology, the aircraft should be designed in a way that facilitates a network of operations with stopovers.

Table 4 Share of CO_2 emissions and number of flights for four different market sizes, as of 2019 and as a fraction of the total amount of commercial passenger transport flights.

	Flights up to 500 km	**Flights up to 800 km**	**Flights up to 1000 km**	**Flights up to 2000 km**
Share of total aviation CO_2 emissions	6%	14%	19%	43%
Share of total number of scheduled flights	22%	41%	52%	82%

E. Aircraft Noise

The societal acceptance of the aircraft depends not only on its impact on the climate, but also on the noise produced. For this study, no detailed noise assessment was performed, with the exception of simple one-equation estimations for propeller noise based on Ruijgrok [44] when assessing the impact of the number of propellers. Therefore, this final section is limited to a qualitative discussion. However, it is important to manage expectations in this regard. After hearing electric cars and small electrically-driven planes, one may expect a large electric passenger aircraft to be quiet compared to a fuel-burning counterpart. But for such aircraft, the propellers are the dominant source of noise, particularly in take-off. And since the electric aircraft weighs two to three times more than current fuel-based turboprop aircraft, it produces substantially more thrust and features more propellers. Likewise, if we compare it to a narrowbody, the MTOM is the same, but the payload is cut in half. This implies that double the amount of movements are required to displace the same volume of passengers. This, combined with the limited excess power after take-off for a steep climb, means that the noise footprint will be a serious challenge for these aircraft if no action is taken.

Fortunately, the use of distributed electric propulsion also opens the space to novel low-noise designs. The aforementioned low disk loading of the propellers reduces the loading noise, and may allow for lower rotational speeds while maintaining an acceptable propeller efficiency. This can significantly reduce thickness noise, which is driven by the tip Mach number. The fact that electric motors can operate at different rotational speeds while maintaining an acceptable efficiency also provides more design freedom in this regard, particularly to reduce noise during take-off and landing—though a gearbox may be more beneficial than a direct-drive configuration if the propeller rotational speeds are too low. During cruise, cabin noise can be reduced by synchrophasing, similarly to conventional turboprop aircraft [45, 46]. And in landing, the combination of a high approach speed, relatively low wing loading, and propeller effects may allow for reductions in airframe noise by using, for example, slotless flaps. Additional research on these topics is required to ensure low-noise operation of large electric aircraft (*Challenge 10*).

V. Conclusions & Outlook: The Hot Potatoes

In this second paper of the two-part paper series, we present the conceptual design of a battery-electric 90-seater using Class-II handbook design methods. The design-space exploration converges on a tube-and-wing design with distributed propellers and a gas-turbine-based reserve energy system. The resulting design features a maximum take-off mass of 76 tons, a vehicular energy consumption of 167 Wh/pax-km, and achieves a useful range of 500 km, 800 km, or 1000 km, for cell energy densities of 300 Wh/kg, 450 Wh/kg, and 550 Wh/kg, respectively. This corresponds to pack-level energy densities of 240 Wh/kg, 360 Wh/kg, and 440 Wh/kg, respectively. On these ranges, the aircraft presents approximately 70% to 80% lower grid energy consumption than eSAF-based alternatives, and 40% to 75% less than hydrogen-based alternatives, respectively. The climate impact in terms of CO_2-equivalent emissions generated in flight, in the production of energy, and in the production of batteries, is substantially lower than for hydrogen, kerosene, or eSAF-based aircraft, and is comparable to land-based modes of transport. These results imply that battery-electric aircraft can, in fact, play an important role in the decarbonization of the aviation sector: replacing flights up to 800 km can reduce the CO_2

emissions of the aviation sector by up to 14%, while further developments in battery technology and operations would allow electric aircraft to tackle the market up to 2000 km range, which is responsible for 43% of all CO_2 emissions. To maximize this decarbonization potential, a shift in the design objectives (compete with narrowbodies vs. enable new forms of mobility) and operations (web-based regional transport using stopovers vs. point-to-point) of electric aircraft is required.

This perspective is contrary to the majority, if not all, of existing literature, including some previous work of the authors. However, although this paper demonstrates feasibility from an aircraft-design perspective, sub-system-level assumptions have been made which need further verification. Throughout this paper, several technical challenges have been highlighted. These so-called "hot potatoes" require further research to ensure technical feasibility at sub-system level. In the order of appearance:

Challenge 1. Wing/battery-pack integrated design, including battery replacement
Challenge 2. Wing structural sizing for aeroelastic and landing loads with batteries in wing
Challenge 3. Design and certification of the reserve energy system
Challenge 4. High-voltage component and system design
Challenge 5. Thermal management system sizing for powertrain components and batteries
Challenge 6. Mass and energy consumption of non-propulsive systems
Challenge 7. Sizing of tail surfaces and control surfaces with distributed propulsion
Challenge 8. Propeller/wing aerodynamic performance in cruise and high-lift conditions
Challenge 9. Battery cell development for large aircraft applications
Challenge 10. Low-noise propeller design for distributed-propulsion aircraft

Future work will focus on these ten research topics. Based on that, a second design iteration can be performed to confirm if, or with what technologies, the aircraft meets the results set out in this study. Readers are also encouraged to confirm or disprove the findings of this work by performing their own Class-II (or higher) design of similar aircraft.

All things considered—technical feasibility, required technology and infrastructure developments, and climate impact—we believe that battery-powered aircraft for commercial air transport deserve at least the same amount of attention as hydrogen, hybrid-electric, and SAF-based propulsion systems. The opportunity that electric aircraft offer to substantially reduce the negative impact of aviation on global warming warrants substantial investments into the maturation of the technological building blocks that enable electric aviation. By developing these technologies, we can make not just evolutionary steps, but also revolutionary steps in the path towards decarbonization of the aviation sector.

Acknowledgments

This research is funded by Elysian Aircraft Company BV. R. de Vries and R. E. Wolleswinkel declare that they have competing interests, and that they have performed this research in an objective way to the best of their abilities. The authors would like to thank Joaquin Exalto for contributions to the figures presented in this paper and Pieter-Jan Proesmans for input and feedback on the calculations of emissions.

Appendices

A. Aircraft Sizing Methods and Assumptions

This appendix provides an overview of the main assumptions and methods used in the conceptual aircraft design study, for transparency and to indicate where the main uncertainties lie in the component modeling.

A. Performance Modeling

The flight-performance constraints of the wing loading/power loading diagram, as well as the mission analysis, are modeled with physics-based point-performance equations as described in Ref. [18]. Two exceptions in this regard are the take-off performance constraint, which is modeled semi-empirically following Ref. [47], Ch. 9, and the landing-distance constraint, which is modeled semi-empirically following Ref. [48], Part I, Ch. 3. Propeller interaction effects were assessed in exploratory analyses using the method of Ref. [18] and were found to have a small positive effect, but are neglected in the conceptual design study presented here for simplicity. The power lapse of the gas turbine with altitude is modeled according to Ref. [49].

B. Mass Estimation

The semi-empirical component mass build-up of Torenbeek [9], Ch. 8 is used. The following paragraphs list additional assumptions and exceptions that are made, or additional data that is required to estimate the mass of components that are not found in conventional fuel-based aircraft. For the powertrain components, the following approach is taken:

- The mass of the gas turbine of the reserve energy system is estimated using turboshaft mass data of Roskam, Part V, Ch. 6 [48], from which the gearbox mass calculated according to Ref. [50] is subtracted. Accessories and fuel system mass are added following Ref. [9]. A gas-turbine efficiency of 0.4 is assumed.
- Propeller mass is estimated based on Ref. [51].
- The assumed efficiencies and specific powers of the components of the electric drivetrain are listed in the table below. These data are based on a combination of public literature and discussions with manufacturers. Note that the battery efficiency is only used as a proxy to estimate the heat load of the battery, since the cell energy density assumed in Sec. III.C already corresponds to the useful energy that can be extracted from the cell at the required C-rate. A direct-drive electric motor, without gearbox, is chosen in this study. Electric motor specific power refers to maximum continuous power, and it is assumed that 20% over-powering is possible for 3 minutes (during take-off).
- For the thermal management system (TMS), a mass of 1 kg is assumed per kW of heat load rejected, based on values reported in Refs. [25, 52]. The spread in values encountered in literature show that this value is highly uncertain and that a more detailed definition of the TMS is required for accurate mass estimates.

Table 5 Efficiencies and specific powers assumed for the components of the electric drivetrain

Component	Efficiency	Specific power [kW/kg]
Electric motor + inverter	0.95	5
Generator + rectifier	0.93	11
PMAD[a]	0.96	20
Battery	0.95	-

[a]Power management and distribution system, including cables, circuit breakers, fuses, buses, and converters.

In addition, the following assumptions are made for other elements of the aircraft's operating empty mass:

- A 10% and 20% reduction in fuselage mass and tail mass are assumed due to the use of composites, respectively, based on Ref. [47]. For the wing, no weight reduction is assumed in this regard. The choice of materials is to be investigated in more detail.
- When estimating the wing weight according to Ref. [9], Ch. 8, the max zero fuel mass is taken as the total aircraft mass excluding battery mass. This is based on the assumption that the battery contributes to a wing bending relief, similarly to fuel. A more detailed structural analysis of the wing is required to verify this approach. Additionally, the 10% reduction in wing mass due to bending relief of the engines as suggested by Ref. [9] is applied, and a 4% wing mass penalty is assumed for the folding wingtips.
- A 50% reduction in hydraulic and pneumatic systems mass is assumed as a consequence of the electrification of aircraft subsystems. For the same reason, a 25% reduction in the mass of environmental control system (ECS) and ice protection system (IPS) are assumed, which may share functions with the TMS of the aircraft. Conversely, a 100% increase in (non-propulsive) electrical system mass is assumed. Further investigation into the electrification of these aircraft subsystems is required to verify these assumptions.

C. Tail Sizing

The horizontal and vertical tail surfaces are estimated based on volume coefficients. For the horizontal tail, a volume coefficient of $(S_{\mathrm{HT}} l_{\mathrm{HT}})/(c_{\mathrm{mac}} S) = 0.9$ is selected. For the vertical tail, a modified volume coefficient of $(S_{\mathrm{VT}} l_{\mathrm{VT}})/(b l_{\mathrm{fus}} D_{\mathrm{fus}}) = 0.07$ is selected. The vertical tail coefficient based on the fuselage projected area ($l_{\mathrm{fus}} D_{\mathrm{fus}}$) instead of the wing reference area (S) is used because initial sizing studies showed that the original formulation based on wing reference area led to unrealistically large vertical tails as a result of the large wing relative to the fuselage in the

case of electric aircraft. Due to the destabilizing effect of the fuselage, its lateral projected area is also considered a more representative parameter for vertical tail sizing than the wing reference area, and the modified volume coefficient was found to present a slightly stronger correlation with the reference data provided in Ref. [48], Part 2, Ch. 8, than the original volume coefficient based on wing reference area. Moreover, for the vertical tail a 30% reduction in area is assumed due to the reduced yawing moments in case of motor failure and possible use of differential thrust for yaw control in distributed-propulsion configurations, based on Ref. [53]. For the horizontal tail, a 10% reduction in tail area was assumed as a result of the low center-of-gravity excursion present in the electric aircraft. A more detailed control & stability analysis of the aircraft is required to verify these claims.

D. Energy Sizing

The energy required for the nominal mission is computed with a time-stepping mission analysis. In addition to the power required for propulsion, the power required for non-propulsive systems such as the environmental control system and avionics is taken to be 3 kW/passenger, based on Ref. [54]. For the thermal management system of the electrical drivetrain, 0.1 kW of power is assumed to be required per kW of heat rejected, which is roughly halfway between the upper and lower bounds estimated in Ref. [52]. For taxi, take-off, and landing, the energy fractions shown in Table 6 are assumed based on Ref. [48], Part I.

Table 6 Energy required for ground phases of the mission, as a fraction of the total energy carried on board.

Mission phase	Energy fraction
Taxi out	1%
Take-off	0.5%
Landing	0%
Taxi in	0.5%

E. Energy Sizing

A symmetric parabolic drag polar, $C_D = C_{D0} + C_L^2/(\pi A e)$, is used to model the drag of the aircraft. The Oswald factor e is computed as a function of the aspect ratio using the correlation presented in Ref. [55], Ch. 40. An increase of +0.025 and a decrease of -0.025 is applied to the Oswald factor of the electric and reference turboprop aircraft, respectively, to model the sensitivity of having a small or large fuselage relative to the wing span. The zero-lift drag coefficient C_{D0} is estimated using the component drag buildup method of Raymer [20]. For the drag buildup, smooth paint is assumed as surface finish and a 5% increase C_{D0} is assumed for miscellaneous (e.g. leakage & protuberance) drag. The fraction of laminar flow and the interference factors assumed for the various aircraft components are given in Table 7. For the extent of laminar flow on the wing, it is assumed that 10% of the wing surface is laminar downstream of the propellers (note that a propeller does not lead to a fully turbulent boundary-layer; see e.g. Ref. [56]), and that 50% laminar flow is achieved on the folding wingtip.

Table 7 Percentages of laminar flow and interference factors assumed in the zero-lift drag buildup.

Component	Percentage laminar flow	Interference Factor Q
Fuselage	15%	1.0
Wing	16%	1.0
Tail	35%	1.03
Motor nacelles	10%	1.5
Landing gear fairing	10%	1.0

Furthermore, for the thermal management system, a drag penalty of 0.17 N per kW of heat rejected is assumed, based on Ref. [52]. Again, the large spread encountered in literature highlights that a more careful assessment of the TMS is required to produce more accurate values of the drag due to heat exchangers.

Finally, the propeller efficiency is estimated by calculating the propulsive efficiency of an ideal actuator disk as a function of the thrust coefficient, and multiplying it by a constant factor $k = 0.88$ representing non-ideal losses. This approach is similar to Ref. [57].

B. Assumptions Made in Environmental Assessment

This appendix lists the main assumptions made in Sec. IV to estimate the grid energy consumption and emissions of various vehicles. For the comparison of energy consumption:

- The fuel-based reference turboprop is designed for the same mission and using the same sizing tool as the electric aircraft, with the same assumptions regarding component technologies.
- For the A320neo-like narrowbody, an energy consumption of 250 Wh per passenger-kilometer is assumed for max payload and short range, based on Refs. [7, 36] and various online sources. The spread in data encountered indicates more reliable sources are required for an accurate estimate.
- For the regional H_2 fuel-cell aircraft, an energy consumption of 300 Wh/pax-km at full payload is selected for an 800 km mission based on Ref. [36], which reports an anergy consumption of 300 Wh/pax-km for a 700 km mission, and 262 Wh/pax-km for a 1480 km mission.
- For the narrowbody H_2 turbine aircraft, an energy consumption of 150 Wh/pax-km at full payload is selected for an 800 km mission based on Ref. [36], which reports an anergy consumption of 138 Wh/pax-km for a 1575 km mission, and 130 Wh/pax-km for a 4445 km mission.
- For all aircraft, an average occupancy of 85% is assumed, which is representative of narrowbody economy class [7].
- For the car (EV), an energy consumption of 152 Wh/km is taken, based on data for a Tesla Model 3 in Ref. [58]. For the EV, an average occupancy of 1.2 passengers and a battery pack capacity of 75 kWh is assumed.
- For the train, an energy consumption of 75 Wh/pax-km is selected, corresponding to the densely-travelled, electrically-powered train network in the Netherlands in 2019 [59].

In order to get a first estimate of the emissions of the various modes of transport, the following assumptions are made:

- The CO_2 emitted in the production of hydrogen, eSAF, or electricity to charge the batteries is computed with the grid energy consumption and a given grid emission index, in grams of CO_2 emitted per kWh of grid energy produced. The spread in grid-to-tank efficiencies shown in Fig. 6 is taken as the uncertainty band. For eSAF aircraft, direct air capture is assumed to be required to achieve a net-zero carbon cycle.
- For conventional kerosene-based aircraft, the energy required to produce kerosene is assumed to be 0.26 kWh per kWh of fuel energy produced, based on Ref. [60]. A generic ±25% uncertainty is assumed on this value. During the combustion of kerosene, 3.16 kg of CO_2 is emitted per kg of kerosene consumed.
- Battery manufacturing: the CO_2 emitted in the production of batteries is difficult to quantify because it depends on where the batteries are made, where the energy comes from, and where the materials come from. Here we assume that 35 to 87.5 kg of CO_2 is emitted per kWh of battery capacity produced, depending on the cleanliness of the energy used. Note that even for a fully-renewable energy source, CO_2 may be emitted in the extraction and chemical transformation of raw materials. These values are based on Ref. [61], assuming a 50% reduction in emissions on a per-kWh basis for a high-energy-density battery (350 Wh/kg) compared to a traditional battery (100 Wh/kg). This assumption may be conservative since it corresponds to a 75% increase in emissions on a per-kg basis for the advanced battery. This contribution to emissions is spread over 1500 cycles with an average range of 700 km per cycle for the electric aircraft (note that the average range is lower than the harmonic range), and over 320,000 km distance in the case of the electric vehicle [58]. Second-life applications and emissions created in the disposal or recycling of the battery are not accounted for. On one hand, a second-life application of equal number of cycles would halve the emissions due to battery production on a per-passenger-kilometer basis. On the other hand, some energy is required to dispose or disassemble the batteries at their true end of life. To be conservative, a ±90% uncertainty is assumed for these values.
- The non-CO_2 effects of aircraft on the climate, such as water vapor and contrails, are particularly difficult to quantify. The work of Lee et al. [37] indicates that in the current aviation system non-CO_2 effects have approximately twice the impact on global warming, compared the CO_2 effects. This factor 2 comes with a 95% confidence interval of ±1.3. Based on this, we assume the following ratios of non-CO_2 effects to CO_2-effects:

- For a kerosene-based, A320neo-like narrowbody: a factor 2, based on Ref. [37]. An uncertainty of ±65% (1.3÷2) is applied based on the 95% confidence interval of Ref. [37].
- For an eSAF-based, A320neo-like narrowbody: an additional 25% reduction with respect to the kerosene-based variant is assumed. This is based on 50% reduced soot emissions and ice-crystal formation [62] leading to an approximately 25% reduction in radiative forcing [63], which is in line with Ref. [6]. We assume the same uncertainty interval width as for the kerosene-based aircraft: while the non-CO_2 contributions of eSAF aircraft are lower than kerosene aircraft and therefore one could expect the error band to be smaller in an absolute sense, there are also additional unknowns with respect to the impact of eSAF on non-CO_2 emissions.
- For the fuel-based reference turboprop: a factor 0.5, since contrails are not generated at the lower cruise altitude and CO_2 effects dominate [64], but NO_x and other emissions are still produced. We apply the same uncertainty interval as above. The same factors are applied for Jet A1 and eSAF, since in this case the reduction in contrails with eSAF is not applicable.
- For hydrogen gas-turbine aircraft: 40% less than the non-CO_2 effects that would occur if the aircraft burned kerosene at the same energy. This mimics the 40% reduction suggested in Ref. [6] if one considers the combined effect of NO_x, water vapor, and contrail/cirrus. To be on the conservative side, we assume a ±90% uncertainty on the non-CO_2 effects.
- For hydrogen fuel-cell aircraft: same approach as for hydrogen gas-turbine aircraft but with a 70% lower value than the kerosene equivalent instead of 40%, due to the reduced contrail/cirrus formation and zero NO_x emissions [6]. Again, to be on the conservative side, we assume a ±90% uncertainty on the non-CO_2 effects.

References

[1] Friedrichs, J., Radespiel, R., Werij, H., and Vos, R., "Accelerating the path towards carbon-free aviation," report of the CoE "Sustainable and Energy Efficient Aviation" (SE2A) and Aeronautics Research Centre Niedersachsen (NFL), 2022.

[2] Mukhopadhaya, J., and Graver, B., "Performance Analysis of Regional Electric Aircraft," International Council of Clean Transportation white paper, 2022.

[3] Staack, I., Sobron, A., and Krus, P., "The potential of full electric aircraft for civil transportation: from the Breguet range equation to operational aspects," *CEAS Aeronautical Journal*, Vol. 12, 2021, pp. 803–819. doi:10.1007/s13272-021-00530-w.

[4] Webber, H., and Job, S., "Realising Zero-Carbon Emission Flight," Aerospace Technology Institute report FZ-0-6.1, September 2021.

[5] Epstein, A. H., and O'Flarity, S. M., "Considerations for Reducing Aviation's CO_2 with Aircraft Electric Propulsion," *Journal of Propulsion and Power*, Vol. 35(3), 2019, pp. 572–582. doi:10.2514/1.B37015.

[6] Fuel Cells and Hydrogen Joint Undertaking, Clean Sky 2 Joint Undertaking, "Hydrogen-powered aviation: A fact-based study of hydrogen technology, economics, and climate impact by 2050," , May 2020.

[7] Graver, B., Rutherford, D., and Zheng, S., "CO_2 emissions from commercial aviation: 2013, 2018, and 2019," International Council of Clean Transportation report, 2020.

[8] Wolleswinkel, R. E., de Vries, R., Hoogreef, M. F. M., and Vos, R., "A New Perspective on Battery-Electric Aviation, Part I: Reassessment of Achievable Range," AIAA Scitech 2024 Forum, Orlando, FL, USA, January 8-12 2024.

[9] Torenbeek, E., *Synthesis of Subsonic Airplane Design*, Delft University Press, 1982.

[10] Bonnin, V., Hoogreef, M., and de Vries, R., "Distributed Hybrid-Electric Propulsion Benefits for Span-Limited Aircraft," AIAA SciTech 2023 Forum, National Harbor, MD, USA, January 23-27 2023. doi:10.2514/6.2023-2098.

[11] European Aviation Safety Agency, "Easy Acces Rules for Air Operations," CAT.OP.MPA 180-182, European Aviation Safety Agency, Cologne, Germany, September 2023.

[12] de Vries, R., and Vos, R., "Aerodynamic Performance Benefits of Over-the-Wing Distributed Propulsion for Hybrid-Electric Transport Aircraft," *Journal of Aircraft*, Vol. 60(4), 2023. doi:10.2514/1.C036909.

[13] Karpuk, S., and Elham, A., "Influence of Novel Airframe Technologies on the Feasibility of Fully-Electric Regional Aviation," *Aerospace*, Vol. 8(6), 2021. doi:10.3390/aerospace8060163.

[14] Monjon, M. M. M., and Freire, C. M., "Conceptual Design and Operating Costs Evaluation of a 19-seat All-Electric Aircraft for

Regional Aviation," AIAA Propulsion and Energy Forum (virtual event), August 24-28 2020. doi:10.2514/6.2020-3591.

[15] Courtin, C., Mahseredjian, A., Dewald, A. J., Drela, M., and Hansman, J., "A Performance Comparison of eSTOL and eVTOL Aircraft," AIAA Aviation 2021 Forum, Virtual Event, August 2-6 2021. doi:10.2514/6.2021-3220.

[16] European Aviation Safety Agency, "Certification Specifications and Acceptable Means of Compliance for Large Aeroplanes (CS-25)," Amendment 27, European Aviation Safety Agency, Cologne, Germany, November 2021.

[17] International Civil Aviation Organization, "Annex 16, Environmental Protection, Volume I – Aircraft Noise," 8th edition, ICAO, Montreal, Canada, 2017.

[18] de Vries, R., Brown, M., and Vos, R., "Preliminary Sizing Method for Hybrid-Electric Distributed-Propulsion Aircraft," *Journal of Aircraft*, Vol. 56(6), 2019, pp. 2172–2188. doi:10.2514/1.C035388.

[19] Finger, D. F., de Vries, R., Vos, R., Braun, C., and Bil, C., "Cross-Validation of Hybrid-Electric Aircraft Sizing Methods," *Journal of Aircraft*, Vol. 59(3), 2022, pp. 742–760. doi:10.2514/1.C035907.

[20] Raymer, D. P., *Aircraft design: A conceptual approach*, 6th Edition, AIAA Education Series, 2018.

[21] Torenbeek, E., "Development and Application of a Comprehensive, Design-senstive Weight Prediction Method for Wing Structures of Transport Category Aircraft," Delft University of Technology, Department of Aerospace Engineering Report LR-693, September 1992.

[22] European Aviation Safety Agency, "Third Publication of Means of Compliance with the Special Condition VTOL," MOC-3 SC-VTOL, Issue 2, European Aviation Safety Agency, Cologne, Germany, June 2023.

[23] Borer, N. K., Patterson, M. D., Viken, J. K., Moore, M. D., Clarke, S., Redifer, M. E., Christie, R. J., et al., "Design and Performance of the NASA SCEPTOR Distributed Electric Propulsion Flight Demonstrator," 16th AIAA Aviation Technology, Integration, and Operations Conference, Washington, DC, USA, June 13-17 2016. doi:10.2514/6.2016-3920.

[24] Lee, H., and Lee, D.-J., "Rotor interactional effects on aerodynamic and noise characteristics of a small multirotor unmanned aerial vehicle," *Physics of Fluids*, Vol. 32, 2020. doi:10.1063/5.0003992.

[25] Biser, S., Filipenko, M., Boll, M., Kastner, N., Atanasov, G., Hepperle, M., Keller, D., et al., "Design Space Exploration Study and Optimization of a Distributed Turbo-Electric Propulsion System for a Regional Passenger Aircraft," AIAA Propulsion and Energy Forum (virtual event), August 24-28 2020. doi:10.2514/6.2020-3592.

[26] Mitchell, G. A., "Experimental Aerodynamic Performance of Advanced 40°-Swept, 10-Blade Propeller Model at Mach 0.6 to 0.85," NASA Technical Memorandum 88969, 1988.

[27] Keller, D., "Towards higher aerodynamic efficiency of propeller-driven aircraft with distributed propulsion," *CEAS Aeronautical Journal*, 2021. doi:10.1007/s13272-021-00535-5.

[28] Argonne National Laboratory, "The U.S. Department of Energy Vehicle Technologies Office and National Aeronautics and Space Administration Joint Assessment of the R&D Needs for Electric Aviation," Argonne National Laboratory white paper, September 2021.

[29] European Comission, "Strategic Research Agenda for Batteries," European Technology and Innovation Platform on Batteries – Batteries Europe, December 2020.

[30] Chin, J. C., Look, K., McNichols, E., Hall, D. L., Gray, J. S., and Schnulo, S. L., "Battery Cell-to-Pack Scaling Trends for Electric Aircraft," 2021 AIAA/IEEE Electric Aircraft Technologies Symposium, Denver, CO, USA, August 11-13 2018. doi:10.23919/EATS52162.2021.9704819.

[31] Viswanathan, V., Epstein, A. H., Chiang, Y.-M., Takeuchi, E., Bradley, M., Langford, J., and Winter, M., "The challenges and opportunities of battery-powered flight," *Nature*, Vol. 601, 2022, pp. 519–525. doi:10.1038/s41586-021-04139-1.

[32] McDonald, R., "Batteries Are Not Fuel," , 2023. doi:10.31224/2803.

[33] Bills, A., Sripad, S., Fredericks, W. L., and Singh, M., "Performance Metrics Required of Next-Generation Batteries to Electrify Commercial Aircraft," *ACS Energy Letters*, Vol. 5(2), 2020, pp. 663–668. doi:10.1021/acsenergylett.9b02574.

[34] The Royal Society, "Net zero aviation fuels: resource requirements and environmental impacts policy briefing," , February 2023.

[35] Agora Verkehrswende, Agora Energiewende and Frontier Economics, "The Future Cost of Electricity-Based Synthetic Fuels," , September 2018.

[36] Debney, D., Beddoes, S., Foster, M., James, D., Kay, O., Karim, S., Stubbs, E., Thomas, D., Weider, K., and Wilson, R., "Zero-Carbon Emission Aircraft Concepts," Aerospace Technology Institute Fly Zero report FZO-AIN-REP-0007, March 2022.

[37] Lee, D. S., Fahey, D., Skowron, A., Allen, M. R., Burkhardt, U., Chen, Q., J., D. S., et al., "The contribution of global aviation to anthropogenic climate forcing for 2000 to 2018," *Atmospheric Environment*, Vol. 244, 2021. doi: 10.1016/j.atmosenv.2020.117834.

[38] European Environment Agency, "Greenhouse gas emission intensity of electricity generation in Europe," , 24 October 2023. URL https://www.eea.europa.eu/en/analysis/indicators/greenhouse-gas-emission-intensity-of-1, accessed December 2023.

[39] European Environment Agency, "CO2-emission intensity from electricity generation," , 30 June 2023. URL https://www.eea.europa.eu/data-and-maps/daviz/sds/co2-emission-intensity-from-electricity-generation-6/, accessed December 2023.

[40] Ledsom, A., "France Legally Bans Short-Haul Flights—Environmentalists Want More," , 4 June 2023. URL https://www.forbes.com/sites/alexledsom/2023/06/04/france-legally-bans-short-haul-flights-environmentalists-want-more/, accessed December 2023.

[41] International Energy Agency, "Global Energy & CO2 status Report: The latest trends in energy and emissions in 2018," , 2019. URL https://www.iea.org/reports/global-energy-co2-status-report-2019.

[42] Schafer, A., and Victor, D. G., "The future mobility of the world population," *Transportation Research Part A: Policy and Practice*, Vol. 34(3), 2000, pp. 171–205.

[43] Antcliff, K., Borer, N., Sartorius, S., Saleh, P., Rose, R., Gariel, M., Oldham, J., et al., "Regional Air Mobility: Leveraging Our National Investments to Energize the American Travel Experience," NASA Report, April 2021.

[44] Ruijgrok, G. J. J., *Elements of Aviation Acoustics*, Delft University Press, 2004.

[45] Pascioni, K. A., Rizzi, S. A., and Schiller, N. H., "Noise Reduction Potential of Phase Control for Distributed Propulsion Vehicles," AIAA Scitech 2019 Forum, San Diego, CA, USA, January 7-11 2019. doi:10.2514/6.2019-1069.

[46] Magliozzi, B., "Synchrophasing for cabin noise reduction of propeller-driven airplanes," 8th Aeroacoustics Conference, Atlanta, GA, USA, April 11-13 1983. doi:10.2514/6.1983-717.

[47] Torenbeek, E., *Advanced aircraft design: conceptual design, analysis and optimization of subsonic civil airplanes*, John Wiley & Sons, 2013.

[48] Roskam, J., *Airplane Design*, DARcorporation, 1985.

[49] Ruijgrok, G. J. J., *Elements of airplane performance*, Delft University Press, 1996.

[50] Johnson, W. R., "NDARC NASA Design and Analysis of Rotorcraft," NASA Technical Publication 2009-215402, December 2009.

[51] Filippone, A., *Advanced aircraft flight performance*, Cambridge University Press, 2012.

[52] Chapman, J. W., Hasseeb, H., and Schnulo, S., "Thermal Management System Design for Electrified Aircraft Propulsion Concepts," AIAA Propulsion and Energy 2020 Forum, Virtual Event, August 24-28 2020. doi:10.2514/6.2020-3571.

[53] Nguyen, E., Alazard, D., Pastor, P., and Döll, C., "Towards an Aircraft with Reduced Lateral Static Stability Using Electric Differential Thrust," 18th AIAA Aviation Technology, Integration, and Operations Conference, Atlanta, GA, USA, June 25-29 2018.

[54] Gnadt, A. R., Speth, R. L., Sabnis, J. S., and Barrett, S. R. H., "Technical and environmental assessment of all-electric 180-passenger commercial aircraft," *Progress in Aerospace Sciences*, Vol. 105, 2019, pp. 1–30. doi:10.1016/j.paerosci.2018.11.002.

[55] Obert, E., *Aerodynamic Design of Transport Aircraft*, IOS Press, 2009.

[56] Howard, R. M., and Miley, S. J., "An investigation of the effects of the propeller slipstream on a laminar wing boundary layer," SAE Technical Paper Series, 850859, 1985.

[57] Zamboni, J., Vos, R., Emeneth, M., and Schneegans, A., "A Method for the Conceptual Design of Hybrid Electric Aircraft," 2019 AIAA Aerospace Sciences Meeting, San Diego, CA, USA, January 7-11 2019.

[58] Tesla, "Impact Report 2019," , 2019. URL https://www.tesla.com/ns_videos/2019-tesla-impact-report.pdf, accessed December 2023.

[59] Nationale Spoorwegen, "Annual Report 2020: Zero-emission enterprise," , 2020. URL https://2020.nsannualreport.nl/annual-report-2020/our-activities-and-achievements-in-the-netherlands/performance-on-sustainability/zeroemission-enterprise, accessed December 2023.

[60] Kolosz, B. W., Luo, Y., Xu, B., Maroto-Valer, M. M., and Andresen, J. M., "Life cycle environmental analysis of 'drop in' alternative aviation fuels: a review," *Sustainable Energy & Fuels*, Vol. 4, 2020. doi:10.1039/C9SE00788A.

[61] Hall, D., and Lutsey, N., "Effects of battery manufacturing on electric vehicle life-cycle greenhose gas emissions," International Council on Clean Transportation Briefing, February 2018.

[62] Voigt, C., Kleine, J., Sauer, D., Moore, R. H., Bräuer, T., Le Clercq, P., Kaufmann, S., et al., "Cleaner burning aviation fuels can reduce contrail cloudiness," *Nature Communications & Earth Environment*, Vol. 2(114), 2021. doi:10.1038/s43247-021-00174-y.

[63] Burkhardt, U., Bock, L., and Bier, A., "Mitigating the contrail cirrus climate impact by reducing aircraft soot number emissions," *Climate and Atmospheric Science*, Vol. 1(37), 2018. doi:10.1038/s41612-018-0046-4.

[64] Thijssen, R., Proesmans, P., and Vos, R., "Propeller Aircraft Design Optimization for Climate Impact Reduction," 33rd Congress of the International Congress of the Aeronautical Sciences, Stockholm, Sweden, September 4-9 2022.